

Review

PEM Fuel Cell Applications in Road Transport

Antonio Nicolò Mancino ^{1,*}, Carla Menale ^{1,*}, Francesco Vellucci ¹, Manlio Pasquali ¹ and Roberto Bubbico ^{2,*}

¹ ENEA, Centro Ricerche Casaccia, Dip. TERIN, Via Anguillarese 301, 00123 Roma, Italy; nicolo.mancino@enea.it (A.N.M.); francesco.vellucci@enea.it (F.V.); manlio.pasquali@enea.it (M.P.)

² Department of Chemical, Materials and Environmental Engineering, “Sapienza” University of Rome, Via Eudossiana 18, 00184 Rome, Italy

* Correspondence: carla.menale@enea.it (C.M.); roberto.bubbico@uniroma1.it (R.B.)

Abstract: Fuel cell electric vehicles represent a possible solution to meet the objectives of the energy transition currently underway, which sees the replacement of combustion vehicles with low environmental impact vehicles. For this reason, this market is expected to markedly grow in the coming years. Currently, the most suitable fuel cell technology for both light and heavy transport applications is the Proton Exchange Membrane fuel cell. This review provides a comprehensive description of the state of the art of fuel cell electric vehicles at different levels: vehicle configuration, fuel cell stack, and all the necessary operation systems. The current advantages and limits of the mentioned technology are highlighted, referring to recent studies aimed at optimizing the efficiency of the system and providing future perspectives.

Keywords: PEM; fuel cells; road transport; BoP; electric mobility; electric vehicle; energy transition; efficiency; stack

1. Introduction

Since the beginning, the automotive industry has developed road transport systems based on internal combustion engines (ICE). Fossil fuels became the essential energy source that allowed road transport in our society. Unfortunately, due to the continuously increasing number of light-duty vehicles (LDVs) and heavy-duty vehicles (HDVs), emissions from the transport sector became a significant component of the share of emissions from fossil fuels, accounting for 23% of the world’s energy-related carbon dioxide (CO₂) emissions [1]. A recent study by the International Energy Agency (IEA) describes the global transport sector’s CO₂ emissions by mode according to the Sustainable Development Scenario, 2000–2070: in 2025, LDV emissions (passenger cars, light commercial vehicles, and two-wheelers) are forecast at 3.3 GtCO₂/year, 43.4% of transport sector emissions, whereas HDVs (trucks and buses) account for 30.3% (2.3 GtCO₂/year) [2]. The increase in greenhouse gas emissions due to transport is faster than the increase in emissions in any other energy-using sector and represents a serious threat for the negative effects on climate change [3]. In addition, traditional road transport contributes significantly to local air pollution [4].

In order to fulfill the targets of the Paris Agreement, it is essential to decarbonize the transport sector. Different policies are being implemented by government institutions. The IEA provides an accessible database with an overview of different regulations [5]. In order to achieve a European carbon-neutral economy by 2050, a European Union agreement was recently officialized, stipulating that from 2035 on, only zero-emission vehicles can be sold [6–8]. As far as heavy-duty transport is concerned, in 2023, the Commission proposed an amendment (still to be approved) to the 2019 regulation on CO₂ emissions standards, setting a 100% zero-emission target for city buses by 2030 and a 90% CO₂ reduction target for trucks by 2040 [9].



Citation: Mancino, A.N.; Menale, C.; Vellucci, F.; Pasquali, M.; Bubbico, R. PEM Fuel Cell Applications in Road Transport. *Energies* **2023**, *16*, 6129. <https://doi.org/10.3390/en16176129>

Academic Editor: Ramon Costa-Castelló

Received: 27 July 2023

Revised: 11 August 2023

Accepted: 13 August 2023

Published: 23 August 2023



Copyright: © 2023 by the authors. Licensee MDPI, Basel, Switzerland. This article is an open access article distributed under the terms and conditions of the Creative Commons Attribution (CC BY) license (<https://creativecommons.org/licenses/by/4.0/>).

To comply with the decarbonization goals, an evolution towards a sustainable transportation system integrated with a sustainable energy production system is required. In order to mitigate emissions, the energy system should rely heavily on renewable energy. Assuming that the transport sector can rely on the availability of this clean energy, electric mobility may represent a possible solution to mitigate emissions [10].

The distinctive patterns of intermittence and unpredictability exhibited by renewable energy sources have introduced significant obstacles to maintaining steady power system operation. This has led to temporal and spatial disparities between energy consumption by end-users and its availability. Consequently, energy storage technology emerges as a viable solution to attain stability and enhance the efficiency of renewable energy utilization [11]. For this reason, the use of hydrogen as an energy vector is gaining more attention, taking into consideration the desirable decoupling of energy production and consumption [12]. Among the many different applications, hydrogen can be profitably used in the transport sector, especially as a complementary solution for electrification, where pure electric vehicles are difficult to implement. For this purpose, fuel cells represent the core technology to allow the propulsion of vehicles with hydrogen as a fuel.

This work will review the present status of fuel cell electric vehicles (FCEVs) technology and give an overview of the principal systems, their configuration, and their characteristics. The state-of-the-art in PEM Fuel cell applications in the automotive sector will also be analyzed.

2. FCEVs Current Status

Different studies highlight several advantages of the application of fuel cells for powering automotive systems [13–15]:

- The efficiency of a FCEV (>60%) is higher than that of ICE-powered vehicles;
- Zero emissions: water and heat are the only by-products;
- Wide range of operating power capabilities for vehicles (20 to 250 kW);
- Autonomy ranges are comparable with market references (over 400 km);
- Low refueling time (<5 min);
- No noise.

Proton Exchange Membrane, or Polymer Electrolyte Membrane (PEM) fuel cell, is the most suitable technology for vehicles, as evidenced by its use in the platforms of the most important FCEV manufacturers, namely Hyundai, Toyota, and Honda [13,16].

In comparison with other fuel cell technologies, the main advantages of PEM fuel cells are their quick start-up process, good cold start capability under low-temperature conditions, high power density, flexible operating range, lightweight compact system, operating temperature range (60–80 °C), and low corrosion [13,17–19].

For the aforementioned reasons, the development and market for FCEVs are expanding. The “Global EV Outlook 2023” [8] outlines the electric vehicle market up to date, including FCEVs. At present, the number of FCEVs has increased by 40% compared to 2021, reaching over 72,000 vehicles globally, of which 80% are LDVs and 20% are HDVs, with the latter portion equally distributed between buses and commercial trucks. In particular, it is interesting to note that the truck segment had a significant increase of 60% only in the last year [8,16,20].

As shown in Figure 1, Republic of Korea, the USA, China, and Japan are the main actors in the FCEV market, respectively, with 40%, 21%, 19%, and 11% of total fuel cell vehicles in their stock. Moreover, Republic of Korea is the leading country for FCEV stock in 2022; strong supporting policies contributed to reaching 15,000 FCEV sales in 2022 (of which two-thirds were sold in Republic of Korea) [8]. The second graph highlights the distribution of FCEV stock subdivided according to application. China is the leading country for HDV applications, with 800 light commercial vehicles (LCVs), 5400 buses, and 7000 trucks [8].

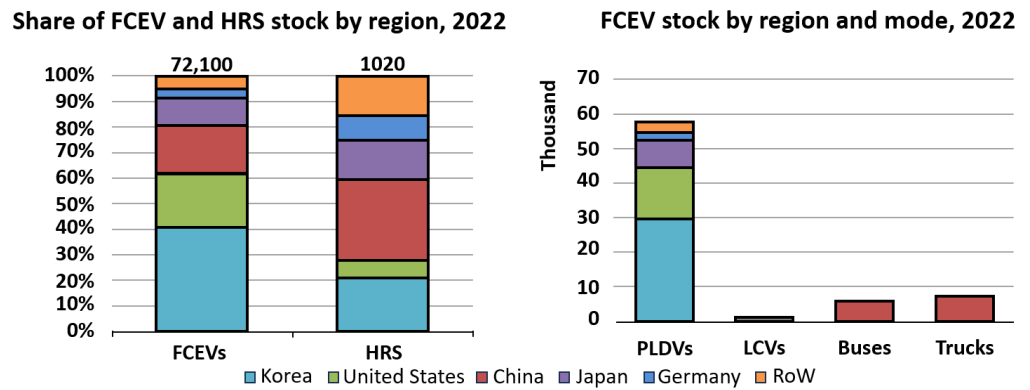


Figure 1. FCEVs and hydrogen refueling station stock by region, 2022. HRS: hydrogen refueling station; PLDVs: passenger light-duty vehicles LCVs: light commercial vehicles; RoW: rest of the world [8].

Despite the mentioned benefits, many aspects of FCEV technology must still be improved. Cost is one of the main obstacles, mainly imputable to the cost of the catalyst inside the fuel cell and the presently unavailable economy of scale due to the small manufacturing numbers [13,18]. The cost of the catalyst, in terms of both raw materials and manufacturing, contributes to about 40% of the total cost of a fuel cell system assembly (Figure 2a) [21,22]. As a reference, the 2025 target cost for a fuel cell system has been set by the US Department of Energy at USD 40/kW, and the ultimate target is USD 30/kW, considering an 80 kW stack with a production volume of 100,000 sets/year and a durability of 8000 h [22,23]. A second drawback is the high operational cost: green hydrogen is still prohibitive (see Figure 2b), and well-to-wheel (WtW) efficiency still presents many losses. The durability of PEM fuel cells in automotive applications is around 2500–3000 h, still lower than the commercial target [24,25]. Again, the catalyst is the most critical component [21,26]. Finally, the absence of an integrated and complete infrastructure, considering its high initial investment costs, represents a real limit to the viability of hydrogen mobility [27].

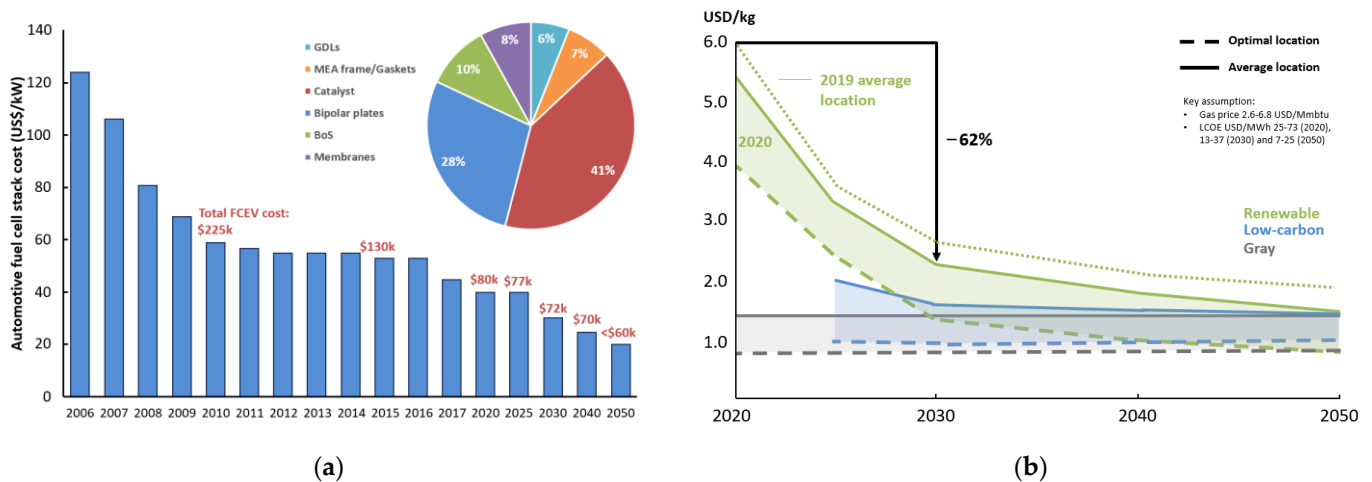


Figure 2. (a) Automotive fuel cell cost evolution and projection. BoS: Balance of Stack; GDL: gas diffusion layer; MEA: membrane electrode assembly [22]. Inset figure: automotive fuel cell component cost distribution based on 500,000 fuel cell systems produced per year; adapted from [28,29]. (b) Hydrogen production costs based on the production method. Adapted from [29].

2.1. FCEVs Configuration

Fuel cell electric vehicles can be classified into two main groups according to the origin of the energy source:

1. All fuel cell vehicles: the traction power is completely provided by the fuel cell. These less-common systems have major disadvantages such as low power response and low power density [21,29,30];
2. Fuel cell hybrid vehicles: the drawbacks of the previous kind of vehicle could be addressed by an onboard integration of energy storage systems (batteries and/or supercapacitors) [16,31]. In this hybrid configuration, the power baseline request is guaranteed by the fuel cell, while all other energy demand (adjusting the dynamic response, peak power demand, starting off, etc.) is given by the electrical energy storage system, which can be charged and discharged based on the power demand and supply. This layout allows the fuel cell to operate at its maximum efficiency [32]. Experimental models are provided with other energy accumulators [33].

Fuel cell hybrid vehicles can be further differentiated into passive and active topologies:

- Passive systems: the fuel cell is directly connected with the battery on the DC bus, implying that their voltages are coupled. No DC/DC converter is used after the fuel cell, and a reduction in its cost can be achieved [32];
- Active systems: typically, a DC/DC converter is used to step up the fuel cell voltage to the battery system voltage, which is usually higher. For complete control and flexibility, an additional DC/DC converter can be used in the connection of the battery to the DC link, decoupling the system operational voltage of each component [32]. Similar topologies can be developed for a supercapacitor [21]. Even if active hybrid systems are more complex in terms of control and configuration, they are much more appealing for their higher efficiency.

In addition, all the previous system layouts should include an additional DC/DC converter to supply power to the BoP and auxiliaries [29]. Figure 3 shows the different configurations.

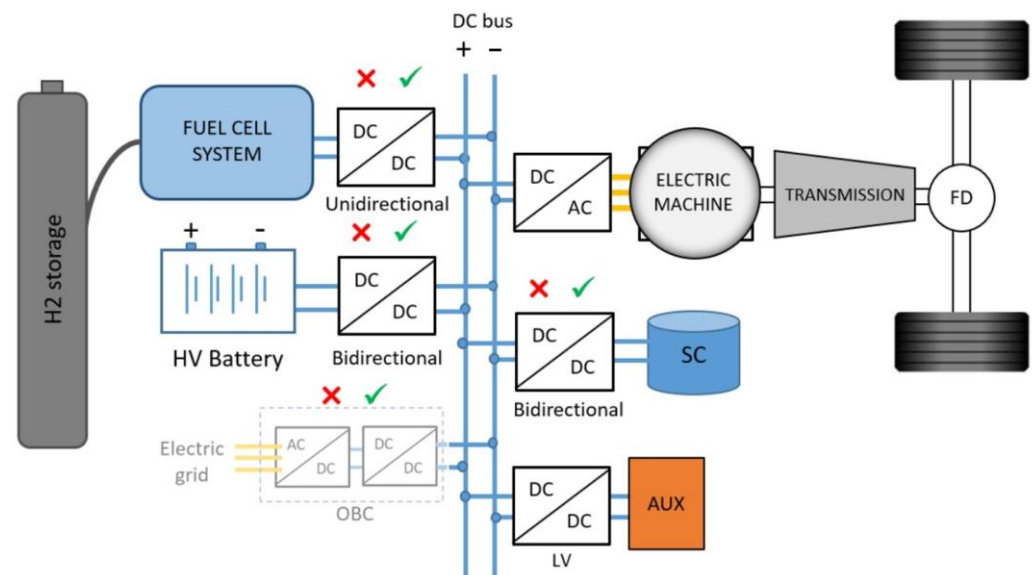


Figure 3. Generic fuel cell electric vehicle (FCEV) powertrain topology, including fuel cell system (FCS), HV battery, electric drive, supercapacitor (SC), transmission, LV auxiliary loads, onboard charger, and related power electronics converters [34].

2.2. Synthetic Comparative Analysis of FCEVs and BEV Technologies

Considering the current diffusion of battery electric vehicles (BEVs), it is important to make a synthetic comparison between the two technologies. Firstly, BEVs and FCEVs are not to be treated as antithetical approaches; their use has different opportunities that may be considered in some way complementary, according to the field of application.

Even if fuel cell vehicles have a higher tank-to-wheel efficiency than ICE vehicles, it is still generally lower than battery electric vehicles: broadly speaking, the average

tank-to-wheel efficiency of ICE vehicles is 25%, while BEVs and FCEVs have an efficiency of 80% [18] and 60% [14], respectively. Considering the very low well-to-wheel efficiency (Figure 4), it is clear that BEVs should be prioritized where possible. It is likely that these issues have also been taken into consideration by the Volkswagen Group in their recently published decision to consistently promote e-mobility powered by batteries rather than hydrogen [35,36]. Moreover, considering typical vehicle driving cycles, batteries are more suitable than fuel cells, which are more prone to degradation [37]. Fuel cells exhibit their highest performance when operating under stable power requirements, preferably at a partial load where efficiency is maximized [32].

Generally, for the small-to-medium vehicle segment, BEV capital and operational costs are lower than for FCEVs [22,38]. Wilken et al. [36] presented a cost comparison for ICE, BEV, and FCEV vehicles, showing that at present FCEV capex, opex, and total cost of ownership are higher and not comparable to BEVs.

However, it must be noted that, with a remarkable increase in shares of energy from renewable sources, hydrogen vehicles can represent an additional chance for BEVs to decouple the non-programmable offer of renewable energy from the power demand [12].

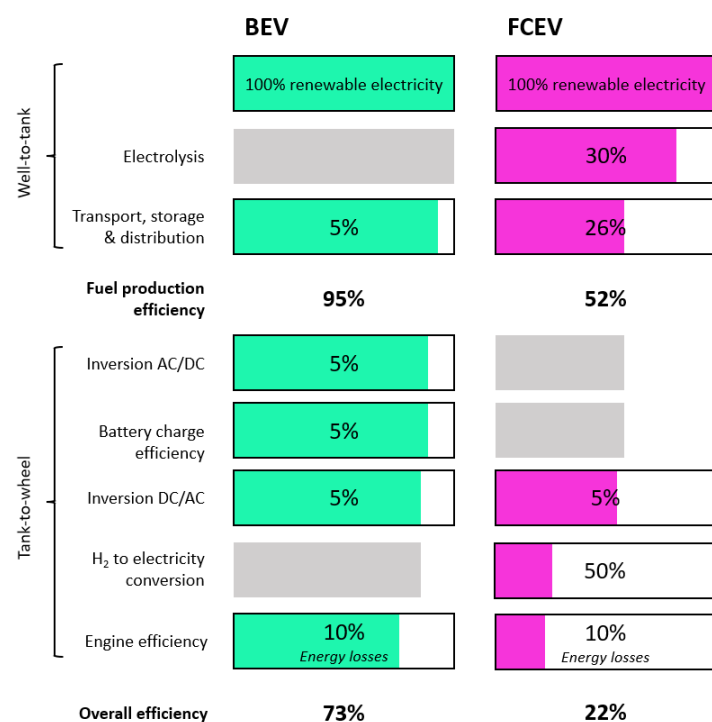


Figure 4. Comparison of the efficiency of two types of powertrains. Adapted from www.transportenvironment.org (accessed on 24 July 2023) [39].

On the other hand, when it comes to applications with elevated power and energy requirements, vehicle weight, and autonomy ranges, hydrogen can be a game changer (Figure 5). Given its higher energy density compared to Li-ion batteries, hydrogen theoretically allows for range extension without adding much weight [39]. Aghabali et al. [40] showed how the use of typical 400 V or 800 V lithium-ion batteries may be limited by the power-to-weight ratio [40,41]. Another point to consider regarding the use of electric vehicles is the enhanced wear of the road surface due to the higher weight and acceleration capacity.

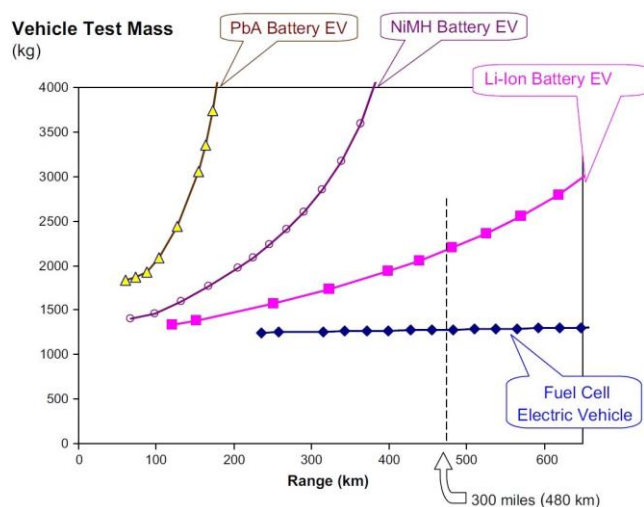


Figure 5. Calculated mass of fuel cell electric vehicles and battery electric vehicles as a function of the vehicle range; the power trains of all vehicles are adjusted to provide a zero to 97 km/h acceleration time of 10 s [42].

Indeed, the use of fuel cell systems in HDVs shows different benefits: an operating cycle more compatible with fuel cells [19]; lower infrastructure costs than other applications, considering the higher level of route predictability and therefore a lower number of refueling stations needed [14]; higher capex allowed due to a more important focus on opex [43]; furthermore, at similar autonomy ranges, fuel cell HDVs have less weight and more space for payload [34]. As an example, Verbruggen et al. [44] showed that a long-haul 40 ton truck with a range of 600 km experienced a minimal reduction in cargo capacity of about 4 tons. This was based on the truck's battery pack energy density of 150 Wh/kg and an average energy consumption of 1.72 kWh/km [34,44]. In contrast, a typical heavy-duty FCEV could travel up to 800 km on a single refueling session. The FCEV accomplished this by using two hydrogen tanks, each capable of storing 40–60 kg of hydrogen at a pressure of 350 bars [34,45].

Another significant positive feature of FCEVs is their consistently shorter refueling times in comparison with BEVs [14]. In addition, there are no resource limitations for platinum considering the future demand, compared to the possible lithium availability constraints in the use of battery electric propulsion for HDVs [46–48].

For the abovementioned reasons, fuel cell propulsion systems are considered more suitable for HDVs such as long-haul transport and machinery/material handling vehicles [21,43].

2.3. Fuel Cell Light-Duty Vehicles

Presently, the leading companies in the FCEV market are Hyundai, Toyota, and Honda. This is inferred by the number of FCEVs recently sold per company: in 2019, Hyundai Nexo accounted for 63% of the total sales, Toyota Mirai for 32%, and Honda Clarity Fuel Cell for around 5% [13,49]. Furthermore, Hyundai's objective for 2030 is to manufacture 500,000 FCEVs per year [50]. All the companies mentioned above are using PEM fuel cells for their vehicles [16,51,52]. In Europe, companies such as Peugeot, Citroën, and Opel are entering the market with new projects for fuel cell vans [16], while others have decided to leave the market, such as the Daimler Group, which, after marketing its GLC F-CELL Hybrid SUV (Plug-In) in 2018, decided not to continue hydrogen car development [53]. Table 1 reports the main characteristics of recent FCEVs.

Table 1. PEM FCEVs models datasheet [15,16,22].

Name	Launch Date	Stack Power [kW]	Fuel Economy [km/kg] (MPGe)	Tank Capacity [kg] @700 Bar (wt%)	Range [km] (EPA)
Daimler GLC FC Hybrid SUV Plug-in	2018	141.6	120 km/kg	4.4	478 + 51 (battery)
Honda Clarity	2016	103	118 km/kg	5	589
Hyundai ix35	2014	100	105 km/kg	5.64	594
Hyundai Nexa	2022	120	119 km/kg	6.33	756
Toyota Mirai	2021	128	116 km/kg	5.6	650

2.4. Fuel Cell Heavy-Duty Vehicles

Manufacturers are gaining familiarity with zero-emission HDVs; currently, twelve models of fuel cell HDV are available on the market, and eight more will be in 2023–2024 [8]. Pardihi et al. [34] listed current and future fuel cell heavy-duty vehicle initiatives.

For public transport, multiple projects and demonstrations are being carried out; see [15,54] as references. A total of 12 European bus OEMs are involved in fuel cell bus transport, and about 1300 fuel cell buses are planned to be deployed in the next few years [15].

Fuel cell technology also shows great potential in the fields of machinery and materials handling [55].

Most of the fuel cell power systems for HDVs, including forklifts [55], utilize compressed hydrogen, stored on board in gas cylinders at pressures up to 350 bar.

Tables 2 and 3 report a selection of fuel cell HDVs with their main characteristics.

Table 2. Selected hydrogen electric truck models [6,56,57].

Name	Stack Power [kW]	Battery Size [kWh]	Tank Capacity [kg] @350 Bar (wt%)	Range [km]
Hyundai-Xcient	190	72	31	400
Daimler-GenH2	300	70	80 liquid	1000
DAF-VDL	60	82	40	400
Kenworth T680 FCEV	310	200	58.8	724
MAN	100	120	34	400
Nikola TRE	200	164	70	805
Scania	90	56	33	500

Table 3. PEM fuel cell electric buses in Europe and the U.S. [15].

Name	Stack Power [kW]	Battery Size [kWh]	Tank Capacity [kg] @350 Bar (wt%)	Range [km]
ACT ZEBRA	120	17.4	40	204
SL AFCB	150	11	50	260
UC Irvine AFCB	150	11	50	244
Businova	30	132	28	190
Streetdeck FCEV (double-decker)	85	48	30	200–265
H2. City Gold	60	29–44	37.5	250
Urbino 12hydrogen	70	30	37.5	220

3. Proton Exchange Membrane (PEM) Fuel Cells

A fuel cell, the core of FCEVs, is an electrochemical system that allows the conversion of the chemical energy stored in hydrogen to electrical energy through a controlled redox reaction. Differently from electrochemical batteries, fuel and oxidants are externally supplied to the system.

Single fuel cell units are composed of [6]:

- A Membrane electrode assembly (MEA), composed of two electrodes separated by an electrolyte, is used for PEM fuel cells. It is a polymer membrane. The electrodes have different layers: the Catalyst Layer (CL) in direct contact with the electrolyte membrane, followed by a Microporous Layer (MPL) and a Gas Diffusion Layer (GDL), both referred to as diffusion media. Typical dimensions and materials are shown in Table 4;

- Gasket: hydrogen is a very small molecule, and the fuel cell environment is particularly harsh; therefore, specific elastomers must be used to avoid gas leakage [58];
- Bipolar plates: thanks to their geometry, they allow the different reactant gases to be fed to the specific electrode. They also have dedicated channels for heat exchange purposes. The bipolar plates enable the electrical connection of more fuel cell units for assembling a whole stack.

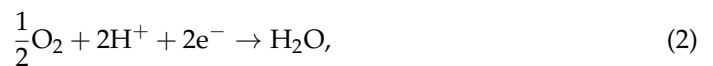
In the case of a direct hydrogen PEM, hydrogen is supplied at the anode while oxygen is provided at the cathode, just canalizing ambient air; to avoid degradation caused by contaminants, pure hydrogen is needed unless specific technology is used [59].

The reactions occurring at the MEA level are depicted in Figure 6a.

Hydrogen oxidation reaction (HOR) at the anode:



oxygen reduction reaction (ORR) at the cathode:



overall reaction:



Under standard conditions, the maximum voltage thermodynamically reachable with one cell producing water in a liquid state as a by-product is given by the Nernst equation:

$$E_0 = -\frac{nF}{\Delta G} = 1.229\text{V}, \quad (4)$$

where:

ΔG is the free Gibbs energy variation (237.2 kJ/mol for the production of liquid water at 25 °C);

n is the number of electrons participating in the reaction;

F is the Faraday constant (96,485 C/mol);

E_0 is the reversible potential of the cell.

Generally, the voltage of a single cell is limited, for physical reasons, to nearly 1 V [60] and is determined as:

$$E_{\text{cell}} = E_0 + \frac{RT}{nF} \cdot \ln\left(\frac{p_r}{p_p}\right), \quad (5)$$

where:

R is the universal gas constant [J/mol K];

T is the temperature in [K];

n is the number of transferred electrons;

F is the Faraday constant [C/mol];

p_r is the partial pressure of reactants [bar];

p_p is the partial pressure of products [bar].

To increase the voltage for common use, a stack of fuel cells may be constructed by connecting multiple units in series [13]. The current collector and end plates complete the stack structure (Figure 6b).

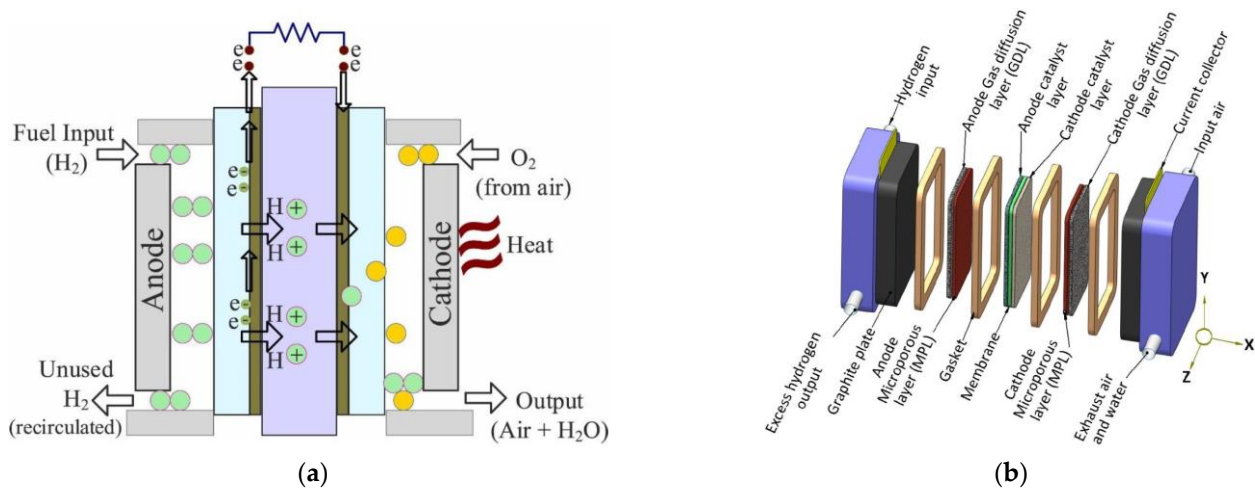


Figure 6. (a) Working principle of a fuel cell unit [61]. (b) Schematics of a fuel cell stack [62].

Table 4. Typical materials of PEM fuel cell components in a stack [63].

Name	Thickness	Density (g/cm ³)	Typical Material
Polymer electrolyte membrane (PEM)	0.01–0.1 mm	~2	Nafion
Catalyst layer (CL)	100 nm–0.05 mm	~0.4	Carbon-supported catalyst and ionomer porous composite
Gas diffusion layer (GDL)	0.1–0.4 mm	0.3–0.5	Carbon fiber-based porous paper
Microporous layer (MPL)	~0.05 mm	0.3–0.5	Carbon black and PTFE binder
Bipolar plate (BP)	0.3–2 mm	1.7–8	Carbon-based composites or materials

3.1. Electrolyte

The main functions of PEM are to separate the anode and cathode reactant gases, ensure proton conductivity from anode to cathode and provide electrical insulation between cathode and anode.

For the above reasons, the material must be impermeable to gases, electrically insulating, and have high ionic conductivity. Furthermore, membranes should have sufficient mechanical resistance and be chemically and thermally stable in their operating ranges [15,63].

The state-of-the-art material for automotive applications is perfluoro-sulfonic acid (PFSA). This material has a main hydrophobic perfluorinated chain, which grants mechanical support and chemical stability, and hydrophilic sulfonic acid end-groups, which facilitate water absorption for proton conduction [63]. The length of those side chains influences the stability and performance of the electrolyte. Long-side chain and short-side chain membranes are mainly different in the number of CF₂ units [15].

During the operation, (H⁺) ions diffuse across the membrane in the form of hydronium ions (H₃O⁺) [63–65]. The proton conductivity is determined by the membrane hydration: when the membrane is too dry, the ionic conductivity is reduced, determining an increase in the ohmic voltage loss; on the other hand, excessive hydration leads to unwanted membrane flooding that hinders the transport of the reactant gases [15,63]. In standard working conditions, the volume and weight of the membrane increase, respectively, by up to 20% and 50%, due to water uptake from the initial dry condition. The optimum hydration level of the membrane depends on different phenomena such as electro-osmotic drag, back diffusion, water generation, and hydraulic permeation across the electrolyte [63].

Dupont's Nafion is the most common long-sidechain PFSA for PEMs. Its characteristics show a proton conductivity of 0.13 S/cm at 75 °C and 100% RH, durability above 60,000 h, and high chemical stability [63]. Wang et al. also illustrated the main fabrication methods.

An example of a short side-chain material for membranes is Solvay's Hyflon. Figure 7 reports the chemical structures of Nafion and Hyflon.

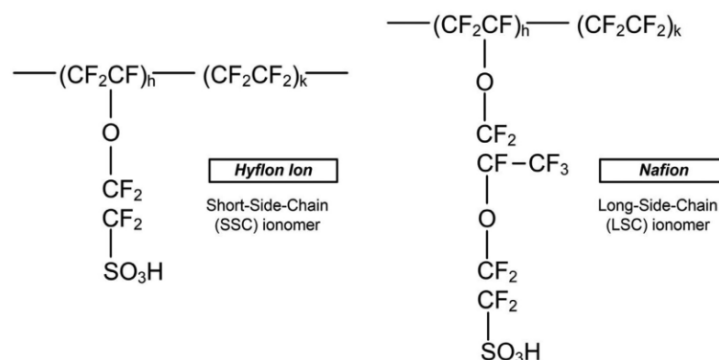


Figure 7. Polymer structures of Hyflon ion/dow, and Nafion [15].

Even if, at present, PFSA is the most commonly used material for PEMs, several drawbacks are still present [13,15,53,66]:

1. Proton conductivity is highly dependent on membrane hydration. This implies the need for accurate humidification control through different strategies (i.e., humidification of reactant gases), which increase system complexity and cost;
2. Temperature limits (around 80 °C) for hydration and mechanical reasons;
3. High production costs;
4. Decomposition of polymer chains due to susceptibility to metallic cations;
5. PEM swell/shrinking during cyclic operation, which can result in membrane failure;
6. Environmentally unfriendly material;
7. Possible degradation of the polymer backbone ($-CF_2-$) for the reaction with hydrogen.

In order to mitigate those problems and extend the operational ranges at low humidity conditions (i.e., 0% RH) and high or low temperatures (i.e., >120 °C), different strategies, reinforcements, or materials have been proposed [15].

Wang et al. [63] provided a review of membrane improvements and production methods, while Wang et al. [15] and Rosli et al. [67] summarized the major alternatives for PEM membrane materials.

A short summary of some interesting solutions is highlighted hereafter: the blend of sulfonated polymers and non-volatile, thermally stable ionic liquids increases ionic conductivity but may decrease mechanical properties; the incorporation of nanoparticles as additives or fillers (graphene oxide, carbon nanotube, silica, polytetrafluoroethylene, ZrO_2 , TiO_2 , $TiSiO_4$, etc.) or the use of different materials such as Sulfonated Hydrocarbon Polymers (polysulfones, polyetheretherketones, polybenzimidazoles, etc.) avoids excessive humidification. Additional strategies are the use of thinner membranes to improve humidification (the transport resistance of protons and water is proportional to the membrane thickness), but they are more prone to mechanical damage and degradation, so reinforcement becomes essential; the use of MPLs to increase water retention; and the use of a counterflow configuration of reactant gases, which improves membrane humidification [63,68].

3.2. Electrodes

3.2.1. Catalyst Layer

Catalyst Layers (CLs) are the electrode surfaces where electrochemical reactions occur. Their role is to facilitate the reactions along with providing pathways for reactant gas supply, water removal, proton transport towards the membrane, and electron conduction towards the current collector [15,63].

A typical CL is composed of catalyst nanoparticles, usually platinum, adsorbed onto carbon particles as support material and impregnated with ionomer thin films, creating a

tortuous void structure with pores [69,70]. The redox reactions take place at these triple-phase boundaries of the CLs [63]. It is essential that the Pt/C powder be mixed with the ionomeric form of the membrane to ensure adequate ionic conduction between CLs and the membrane. There is a precise Pt/C/ionomer equilibrium value: a large quantity of ionomer can reduce the gas diffusion pathways and the contact with the catalyst [71]. Wang et al. [63] determined an optimum Nafion loading of around 30 wt%.

Usually, those blends come in the form of ink/paste that can be deposited either on the membrane or the diffusion media surface. Several methods, such as spraying, screen printing, painting, decaling, rolling, electro-deposition, impregnation reduction, and evaporative deposition, have been used and studied [72].

Even if, due to its high activity, Pt is considered the state-of-the-art material as a PEM catalyst, it has several drawbacks, such as its high cost and poisoning susceptibility to pollutants like CO, which progressively reduce the catalytic performances [13,63,73,74].

Research efforts are focused on improving CO tolerance and reducing the high-cost platinum loading without affecting the durability of the cell using less expensive valuable metals such as ruthenium or palladium, several Pt alloys (Pt-Co, Pt-Ni, Pt-Fe, Pt-V, Pt-Mn, and Pt-Cr) [63], or using cheaper metals [75]. Figure 8 shows the cost and loading targets of platinum catalysts for a 100 kW FCEV, while Table 5 reports the main catalyst alternatives along with their related benefits and drawbacks. For a specific, in-depth analysis, see [13,15,63,70,76–81].

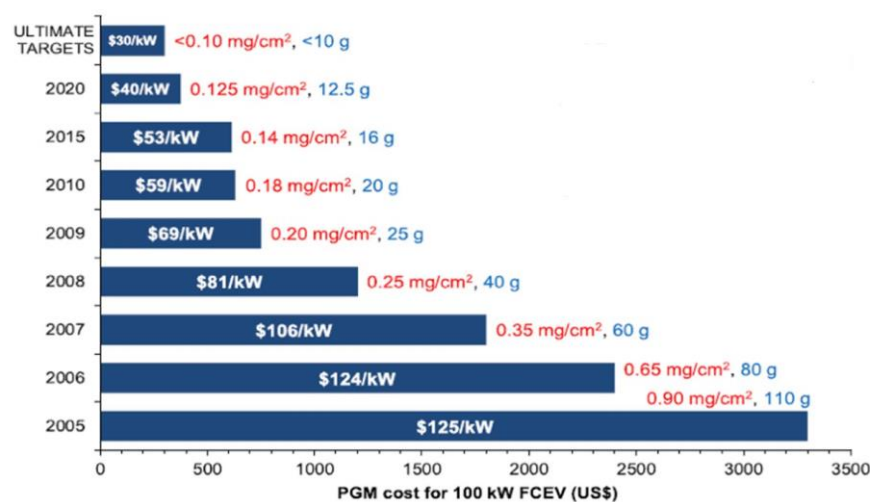


Figure 8. Cost and loading of platinum group metals (PGM) for 100 kW FCEV from 2005 to 2020, based on the current Pt raw price of USD \approx 30/g. The values inside the bars show the total fuel cell stack cost for a manufacturing volume of 500,000 units per year. The values outside the bars give the total catalyst loading per unit cell area (mg/cm^2) and for a 100 kW FCEV (g). Adapted from [13].

Table 5. Benefits and remaining challenges for each of the primary categories of electrocatalysts [15]; ECSA: electrochemical surface area, is the active area of the catalyst where reactions occur. Mass activity is defined as the current at a specified voltage per given mass loading of catalyst; PGM: platinum group metals.

Catalyst-Type	Benefit	Remaining Challenges
Platinum	Mature technology.	Unable to meet long-term automotive Pt loading and catalyst layer durability targets.
Pt alloy/de-alloy	Mature technology;	Difficult to meet the long-term automotive Pt loading target.
	Improved performance over Pt/C; Enhanced MEA durability.	

Table 5. Cont.

Catalyst-Type	Benefit	Remaining Challenges
Core-shell *	Improved mass activity over Pt alloy;	Difficult to maintain the quality of the shell;
	Improved durability over Pt/C;	Dissolution of the core is still a concern.
	Highest reported ECSA.	
Shape controlled nanocrystal	Significantly higher mass activity ($\sim \times 15$) over Pt;	Scale-up is at an early stage;
	Chemical synthesis (vs. electrochemical) may allow for easier scale-up vs. core-shell.	Conflicting data on stability;
		MEA performances have not been demonstrated yet.
Nano-frame/nano-cage **	Significantly higher mass activity ($> \times 20$) over Pt;	Scale-up is at an early stage;
	Highly stable (improved durability over Pt/C).	Ionomer penetration into the nanocage will likely be difficult;
		MEA performance at high current density may be challenging.
Non-precious metal catalyst	Potentially offer the largest benefits (significant cost reduction);	Close to meeting targets for non-automotive applications but far from automotive targets;
		At current volumes, PGM loading is not a major concern for
	Tolerant to common contaminants.	non-automotive applications.

* Core-shell: nanostructures composed of catalyst nanoparticles protected by a porous shell used to prevent their migration and coalescence during the catalytic reactions while still allowing free access to chemical species.

** Nano-frame/nanocage: structural configuration of nano-catalysts similar to porous cage structures or nano-frames.

3.2.2. Diffusion Media

The role of the diffusion media layers is to provide electron conduction between the bipolar plate (BP) and the CL, uniform and direct passage for reactant gas distribution, by-product removal, mechanical support for MEA, and protection of the CL from corrosion and erosion [63]. It must be noted that at the GDL surface, accumulation of water droplets may hinder the reactants flow; therefore, a proper water removal strategy is needed, and the presence of a diffusion media layer is part of it [15].

Carbon paper, made of about 7 μm -diameter fibers aggregated with a binder, is the state-of-the-art material used for GDLs. In order to allow effective water removal, compounds such as Polytetrafluoroethylene (Teflon) are often added to GDL to provide hydrophobic behavior. However, excessive loadings should be avoided; otherwise, the pore volumes will be reduced and gas passage through the pores will be limited. New developments are focusing on metallic and Porous Silicon GDL [63].

A Microporous Layer (MPL) is often inserted between GDL and CL to offer protection for the catalyst, provide a better and smoother physical interface between layers, improve multi-phase contact [63], and improve MEA chemical and mechanical stability [15]. It also has beneficial effects on water management, resulting in reduced ohmic losses (see Zhang et al. [82] for an in-depth study on the influence of MPL on water management). MPL is usually made of carbon black powder bound together with PTFE, which makes MPLs hydrophobic and provides a porous structure with pore dimensions greater than the voids of CLs but smaller than those of the GDL [15,83].

3.3. Bipolar Plates

BPs positioned after the MEA layers allow the series connection of different cells to form a stack, acting as a current collector and giving mechanical support. Their structure, with three different and separated channelings grooved in the surfaces, supplies reactant

gas to each cell as well as the liquid coolant flow. Water removal is performed through the same channels, which should be more hydrophilic than the other layers [15].

The state-of-the-art material for BPs is graphite, which shows good corrosion resistance and good electrical conductivity. On the other hand, graphite is brittle, causing problems during production, and gas permeable, leading to possible leakages [15,63].

Research is exploring several alternative materials, such as carbon composites, which show good electrical and thermal conductivity but weak mechanical robustness, and metals (aluminum, stainless steel, and titanium), which have good mechanical, electrical, thermal properties, and easy machining. In the case of metals, protective coating is needed due to their susceptibility to corrosion, which leads to the formation of oxidants, passive layers, and metal ions that can harm the integrity of the MEA [6,63,84]. Wang et al. [15,63] collect different studies on these new solutions.

Another important aspect is the BP's flow field (channeling) design. It can influence pressure losses and the uniformity of gas spreading, as well as electrical current and heat transmission. Straight parallel rows, serpentine, pin-type, and interdigitated-type flow fields are the most common designs used in PEM fuel cells (Figure 9). Different studies performed an evaluation of several BP flow field geometries [6,15]:

- Parallel: low pressure drops, homogenous distribution of reactants, low water removal capacity, and voltage instability;
- Interdigitated: high water removal capacity, homogenous distribution of reactants, and high pressure drops;
- Pin-type: low pressure drops, low water removal capacity, and uneven distribution of reactants;
- Spiral: low humidity requirements and high pressure drops;
- Serpentine: high water removal capacity, uneven distribution of reactants, high pressure drops.

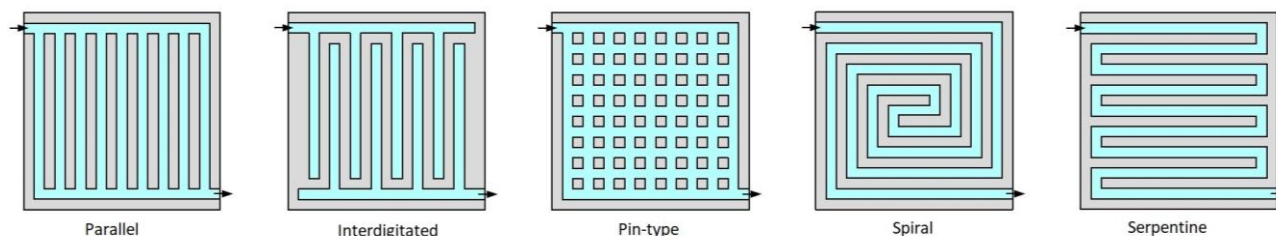


Figure 9. Main flow field designs for bipolar plates [85].

As device power increases, electrode and BP sizes also tend to increase. However, using larger electrodes can lead to problems like uniformity issues in reactions, causing uneven current distribution and potentially forming high-current density hot spots that raise temperature and damage the membrane. This degradation shortens cell and system lifetimes. Hence, BPs must withstand current density variations and be able to distribute appropriate current across the electrodes to counter degradation effects [86].

4. BoP of Fuel Cell Systems in FCEVs

The operation of a fuel cell stack depends on a series of auxiliary systems and components generally referred to as Balance of Plant (BoP). The BoP is composed of three main sub-systems [87]:

- Air supply system: Generally consisting of a compressor, a humidifier, and an air filter. This subsystem provides air to the cathode of the fuel cell;
- Hydrogen supply system: Generally consisting of a tank, a pressure control valve, a recirculator, and purge valves. This subsystem provides hydrogen to the anode of the fuel cell;

- Temperature management system: Generally consisting of a pump, a thermostatic valve, a radiator, and a heater. The circuit is connected to appropriate exchange surfaces in specific channels of the cells' bipolar plates.

Schematization of the fuel cell BoP with the representation of the sub-systems and their components is reported in Figure 10.

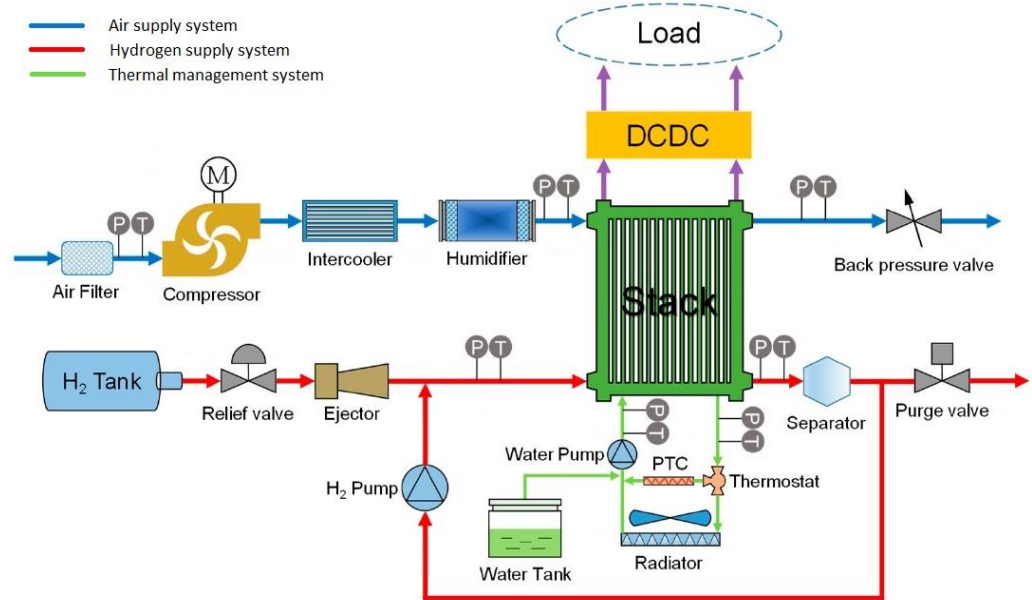


Figure 10. Schematic diagram of the BoP of the PEM fuel cell stack [87].

In vehicle applications, BoP is of key importance considering the limited space and the reliability and affordability requirements of the system.

Recent research in the automotive field [88,89] shows that BoP power consumption, which varies according to the load and operating conditions, can be of the order of 10% compared to the LHV (Lower Heating Value) of hydrogen. Overall, the total cost of the BoP is estimated to represent approximately 56% of the total cost of the fuel cell system [28]. Figure 11 shows the percentage cost distribution of the BoP components in a fuel cell system.

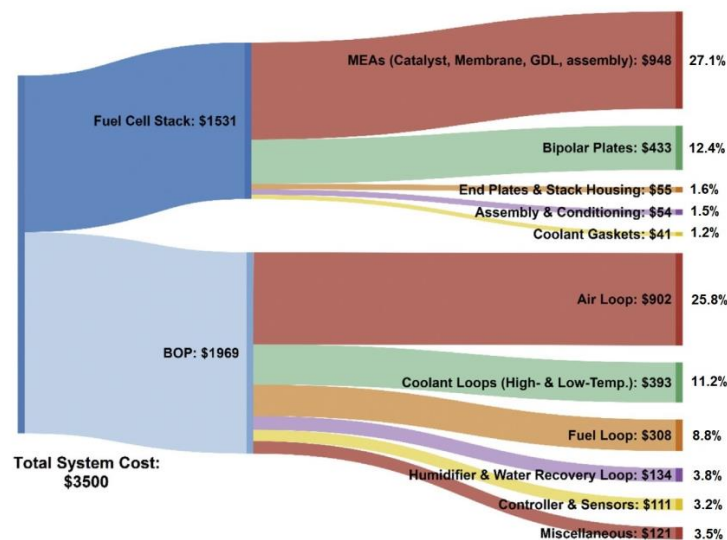


Figure 11. Component cost breakdown at a production volume of 500,000 units/year for fuel cell systems; 2017 updated. Adapted from [28].

4.1. Air Supply System

FCEVs generally use ambient air to obtain the oxygen needed for the reaction with the hydrogen in the fuel cell. In order to improve the performance of the system, the operation is performed in a pressurized condition, generally around 1.5–2.5 bar [90,91]. An increase in the air pressure is beneficial from different points of view [13,91–93]:

- According to Nernst Equation (5), pressurizing the air inlet increases the voltage and thus the power of the fuel cell. However, beyond 4 bar, the voltage increase will be smaller due to mass transport constraints;
- It reduces the stack volume;
- A higher pressure will result in a higher oxygen concentration with reduced polarization in bulk transit, thus improving the kinetics of the reaction and finally allowing a higher efficiency;
- Improved gas transport and water management, with a reduction in membrane degradation.

One of the main problems related to oxygen supply to the fuel cell is oxygen starvation. Gas supply lag due to a sudden fluctuating load (e.g., start-stop or quick change in working conditions) can cause oxygen shortages in the stack. If this condition occurs even in a single cell, it will be forced by the other cells to operate at the same current. Therefore, it will start to operate in voltage reversal conditions (electrolytic mode) with the energy provided by the other cells. This anomaly will deteriorate the catalyst and seriously damage the cell [94,95].

Excess air supply, $\lambda > 1$, is a solution to mitigate this problem. The air excess ratio, lambda λ , is defined as the ratio of actual oxygen flow into the stack to the consumed oxygen flow [92]:

$$\lambda = \frac{\dot{m}_{\text{air}}}{\left(\frac{I \cdot n \cdot M_{\text{air}}}{4 \cdot F \cdot x_{\text{O}_2}}\right)}, \quad (6)$$

where

\dot{m}_{air} [kg/s] is the air mass flow flowing through the cathode;

I [A] is the stack current;

n is the number of cells in the stack;

M_{air} [g/mol] is the molar mass of air;

F [C/mol] is the Faraday constant;

x_{O_2} is the mole fraction of oxygen in air.

On the other hand, the increase in the air excess ratio will increase the power consumption of the air compressor due to more demanding conditions, reducing the net power output [94,96]. Therefore, a proper balance has to be found; generally, the ratio for the optimal operation of PEM fuel cells is $\lambda \approx 2$ [91,97]. In order to achieve proper pressure, a compressor with a compression ratio of ≈ 2 –3 is needed [93].

Operating parameters of the air compressors strongly influence the fuel cell and system efficiency [92], being the component of the BoP with the highest power consumption, up to about 30% of the fuel cell output power [91,98].

Three different layouts of the air compression stage are considered in fuel cell applications (Figure 12) [91–93,99]:

1. Single stage connection: one compressor and an eventual throttle valve after the stack to control an additional increase in pressure;
2. Turbocharger: one compressor and one expander (turbine). This combination can recover 20–50% of the power consumed by the compressor;
3. Two-stage serial compressors: a second compressor is used to boost the compression of the first one.

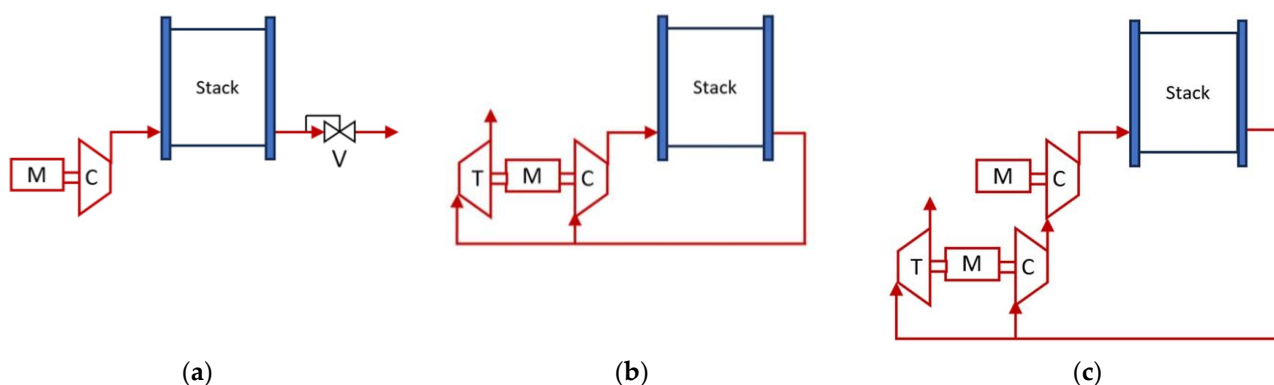


Figure 12. (a) Single-stage compressor (either positive displacement or centrifugal); (b) combined compressor and expander; and (c) two-stage serial turbocharger (M: motor; C: compressor; and T: turbine) [93].

The turbocharger layout shows the greatest potential, being compact, light, and having high efficiency [30,91]. Similar components are also used in ICE vehicles, but the operating conditions are very different: for example, in PEM fuel cells, the exhaust stream is at 80–120 °C, while in typical ICE turbines, the exhaust stream is at about 950 °C. Thus, developing compressors with high efficiency for these applications and implementing an optimal layout are essential [91,92]. The main kinds of expanders for PEM fuel cells currently include screw-type, root-type, scroll-type, and turbine-type [91]. Many studies suggest centrifugal turbo-compressors and root compressors/expanders as the two main possible compressor kinds for FCEVs use, with the first being the most common. They have high efficiency, compact size, and reduced cost, though with some constraints such as surge, pulsation, and a narrow operation range [91,93].

Many research activities are focusing on the study of different types of controllers based on different measures and algorithms to grant optimal working conditions and prevent compressor damages due to overheating, high pressures, and pressure fluctuations [91,92,94].

Water management is a crucial aspect of fuel cell operation and is largely influenced by the working condition of the air supply system. At low supply air velocity, a higher tendency for water accumulation will occur, leading to flooding as well as problems linked to oxygen starvation. With increasing air mass flow, the air pressure will increase, and the stack voltage will rise. Water removal will also be facilitated; however, membrane drying-up problems may occur after long operation at high air mass flow [92].

The system must be tuned according to its characteristics to find a proper balance, even with the possible use of a humidifier that can be installed in the air supply system in addition to the compressor. On FCEVs, the restricted amount of space available for transporting water for humidification may require the installation of a humidification system with internal or external water recirculation (as used in the Toyota Mirai) [13,63].

The most popular humidifier technologies are water bubblers, where the temperature of the liquid is controlled and hence the relative humidity (RH) of the passing gases [63]. Recent studies are examining the use of membrane humidifiers, so self-humidification is becoming more and more interesting thanks to new membrane technologies [68,93].

Finally, the air supply system should also include a filter. Rojas et al. [100] reported that bad air quality may reduce fuel cell efficiency due to particle and compound accumulation in the stack membrane [13].

4.2. Hydrogen Supply System

Hydrogen has a very low volumetric density, and therefore having sufficient onboard storage capacity in order to grant autonomy ranges similar to those of ICE vehicles is

challenging in terms of weight, volume, safety, and cost. Different approaches have been proposed [13]:

- Compressed hydrogen: Generally, FCEV manufacturers implement this method to store hydrogen onboard. Pressure can vary between 350 and 700 bar according to the application and technology. To reach those values, around 15% of the lower heating value of hydrogen must be spent in the process. At those pressures, the capacity to provide a driving range similar to ICE vehicles has already been shown in Tables 1–3. Compressed hydrogen is usually contained in carbon fiber-reinforced plastic composites vessels [13,63];
- Liquid cryogenic hydrogen: To keep hydrogen in a liquid state at atmospheric pressure, a temperature of $-253\text{ }^{\circ}\text{C}$ must be reached and assured for the whole storage duration [101]. The density of liquid hydrogen is 71 kg/m^3 at 1 bar and 20 K, which is much higher than the 40 kg/m^3 of H_2 compressed at 700 bar and 288 K [63]. Even if a high-pressure system can be avoided, this method shows different disadvantages, such as higher energy consumption (more than 30% of the heating value), boil-off losses, high costs, and limited storage time [13]. Liquid hydrogen must be contained in properly insulated vessels [63]. To achieve the desired driving range for a wide variety of light-duty vehicle models, it will be necessary to have onboard hydrogen storage capabilities ranging from 5 to 13 kg of hydrogen [102];
- Metal hydride: This method provides high storage capacities on both a gravimetric and volumetric basis. Hydrogen molecules are stored in the chemical structure of either binary hydrides, composed of a single metal, or intermetallic hydrides, containing multiple metals [103]. Common examples are Alane (aluminum hydride, AlH_3), lithium borohydride (LiBH_4), and sodium borohydride (NaBH_4) [63]. The principal advantages of this technology consist of its compactness and a reduction in refueling costs of around 36–39% [55,103,104]. The main drawbacks of this approach are the heavy storage devices required (even though in some cases they can be used as ballast) [55], the low hydrogen release rate, the higher refueling time, and the high temperatures/pressures necessary for reversible operation [63]. However, thermal integration may be achieved: hydrogen absorption and desorption are associated with the release/absorption of large amounts of heat; hence, it is possible to use up to 40–45% of the heat produced by the fuel cell during the operation to improve the overall system efficiency [55,105,106];
- New hydrogen storage approaches are being explored using metal organic frameworks (MOFs), but they are still at an early stage of research [13].

The hydrogen pressure at the fuel cell inlet, typically 1.1–3 bar at a temperature 40 to $85\text{ }^{\circ}\text{C}$ [107], is controlled by an electric pressure control valve [92]. For optimal functioning, fuel cell stacks typically require an over-stoichiometric ratio of fuel supply at the anode, approximately $\lambda_{\text{H}_2} \approx 1.2$, to ensure that the fuel cell has always enough hydrogen available for the electrochemical reaction [107]. In fact, a lack of hydrogen on the anode side can cause voltage reversal, leading to the collapse of the catalyst carbon carrier, corrosion perforation of the carbon paper and bipolar plate, and even scrapping of the cell. This phenomenon, known as hydrogen starvation, is analogous but more harmful than oxygen starvation on the cathode side [95].

In order not to lose precious fuel due to oversupply and to improve water management [94], the system works in Dead End Anode (DEA) mode [108], and the recirculation of unreacted hydrogen is essential [13]. Pressure losses in the fuel cell imply the necessity of pressure control for the recirculation; to this end, active recirculation can be carried out using a blower. This component contributes to the vast majority of the energy consumption of the fuel supply system; moreover, among the BoP components, the blower's power consumption is in second or third place after the air compressor and the coolant pump (around 0.9 kW for an 80 kW fuel cell) [92,108,109]. As an alternative, a passive recirculation system based on a jet pump can be used. This method reduces power consumption, increases

efficiency, and is preferred for its simple structure, high reliability, and low cost [94,110,111]. The two approaches are shown in Figure 13.

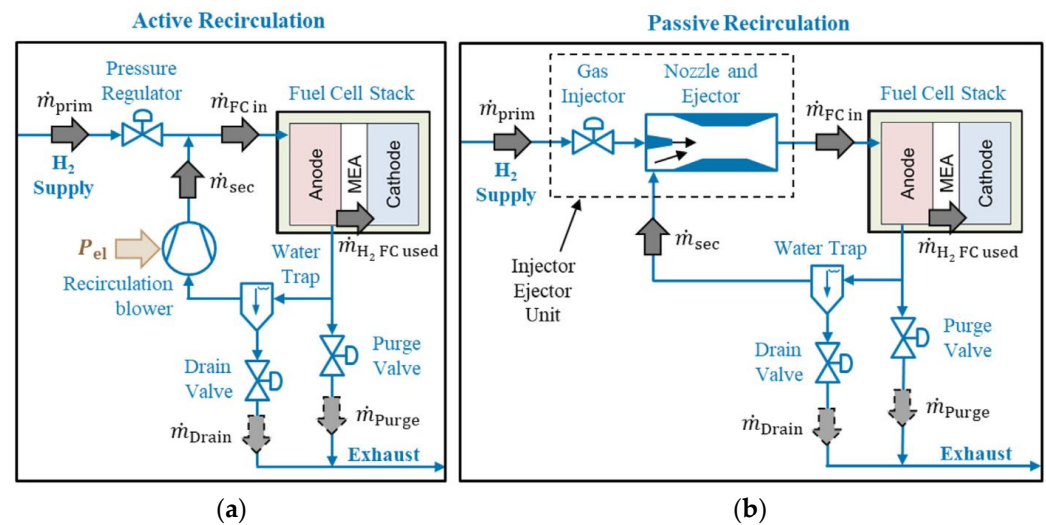


Figure 13. Anode subsystem of a PEM fuel cell: (a) active recirculation and (b) passive recirculation [107].

As described in Figure 14, the primary hydrogen flow passes through a nozzle and provides the kinetic energy for suction. The secondary hydrogen flow, which must be recirculated, enters the suction chamber, is mixed in the mixing chamber with the primary flow, and exits the jet pump through a diffuser [107].

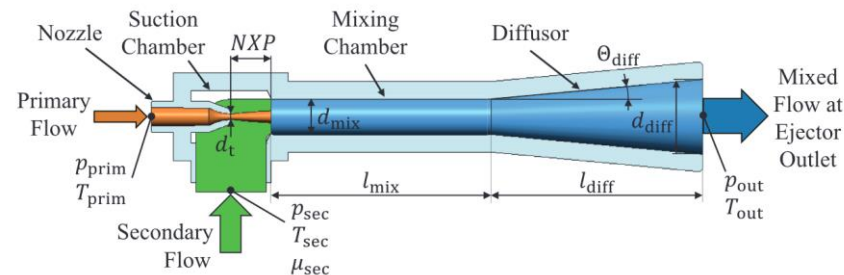


Figure 14. Jet pump working principle [107].

With this technology, complex fluid interactions must be taken into account, making the control of hydrogen supply more difficult [107]. Yin et al. [94] listed many studies addressing the ejector recirculation system, including operating parameter optimization to improve general efficiency. At present, this is the most commonly used technique in FCEVs (differently from the Toyota Mirai, where active recirculation with a blower is installed) [107].

The control of the hydrogen supply system, which is strictly linked to the air supply system, also has an important impact on stack water management. Different chemicals reaching the anode by diffusion mechanisms, such as air nitrogen buildup in the cell or fuel impurities, can deteriorate the stack and reduce its voltage [108]. Under DEA operating mode, water and impurity accumulation in the membrane also contribute to a voltage drop [16,20,108].

Usually, the hydrogen supply pressure at the anode is higher than the air supply pressure at the cathode to limit the migration of nitrogen and the permeation of water vapor through the membrane [88].

A widely used approach to reducing those problems is purging the anode channel. Different purging strategies are proposed in several studies where triggering criteria for the hydrogen purge are defined. Under higher humidity conditions, an adequate triggering value markedly influences stack efficiency, whereas under dry conditions, the purging triggering values do not have a significant impact on efficiency [108].

Hydrogen for automotive fuel cell systems is usually not externally humidified [92].

4.3. Temperature Management System

Assuming an average efficiency of the fuel cell stack of about 60%, the remaining 40% is dissipated as waste heat, produced at a rate proportional to its power output [112].

The heat transfer in PEM fuel cells is characterized by a complex non-isothermal two-phase flow (liquid water and vapor). Chen et al. [112] performed a study on the different heat sources in PEM. The major contributors are the irreversibility of the electrochemical reactions due to the presence of the overpotential in the CLs (up to 60% of the total heating); entropic heat arising from the entropy change in the electrochemical reactions (up to 30% of the total heating); and joule heat resulting from both the ionic and electric resistances (up to 10% of the total heating) [112].

Such an amount of heat greatly influences the performance of a fuel cell, which strongly depends on the working temperature and temperature distribution in the membrane [12,113]. Temperature management is also strictly linked to water management, which also greatly influences the efficiency of the cell.

Optimal working conditions involve two main requisites:

- A nearly constant temperature of about 80 °C: Membrane hydration strongly depends on saturated steam pressure, which is an exponential function of the temperature. Excessive temperature may give rise to membrane dryness, resulting in high ionic resistance, ohmic losses, and material degradation. Meanwhile, low temperatures facilitate the formation of liquid water products, with a higher risk of electrode “flooding”, oxygen starvation, and large mass concentration polarization. Furthermore, it hinders the CL’s electrochemical reaction kinetics and the membrane’s proton conductivity [112];
- Isothermal conditions over the cell area: An uneven temperature distribution in the stack may cause local water phase changes, altering the local relative humidity. However, most importantly, it causes different electrochemical reaction rates across the system. This will finally result in scarce utilization of the catalyst and the reactants, as well as the creation of hot spots, which can lower efficiency and endanger the durability of the fuel cell [113].

Under stoichiometric conditions, a small amount of heat (<5%) can already be removed just by the reactant gas flow. This is not enough to adequately cool down the stack in most cases, but increasing the air stoichiometric ratio can be sufficient to remove the heat and maintain good operation conditions for fuel cells < 100 W. However, for automotive applications, where higher power is needed, this is not sufficient, and in order to meet operative requirements, a proper heat dissipation system is required [112]. Moreover, it must be considered that waste heat removal in a fuel cell system is way more difficult than in ICEs due to the lower base temperature (engine surface temperature of 400 °C vs. the 80 °C of the fuel cell stack) [63]. To this end, different technologies can be used.

Air cooling is the simplest approach. Heat removal is performed on the bipolar plates, where dedicated coolant channels, separated from air and hydrogen channels, are specifically designed. In the case of air cooling, air is forced through a fan to achieve thermal dissipation. This approach can only be applied to small fuel cell systems <2 kW. Liquid cooling is the most common design for PEM fuel cells due to its advantages of large cooling capacity, heat removal efficiency, and flexible control. Liquid is circulated in the cooling channels integrated into BPs using a pump. The most frequent coolants are deionized water (for its high specific heat) and an antifreeze liquid, such as a mixture of ethylene glycol and water. The disadvantages of this technology may be represented by the power consumption of the coolant pump, possible leakages, and corrosion [112].

Many variables may influence the efficiency of the thermal exchange: channel layout and size, which cannot be too small to avoid excessive power consumption; manifold size, which cannot be too large to avoid non-uniformities; flow rate of the coolant, etc. [113]. For automotive applications, both the Toyota Mirai and Hyundai Nexo use one cooling unit per cell in their stacks, while the Honda Clarity uses one cooling unit every two cells to

decrease the stack volume [112]. Figure 15 shows the design of the coolant channels in the Honda FCX Clarity Fuel Cell.

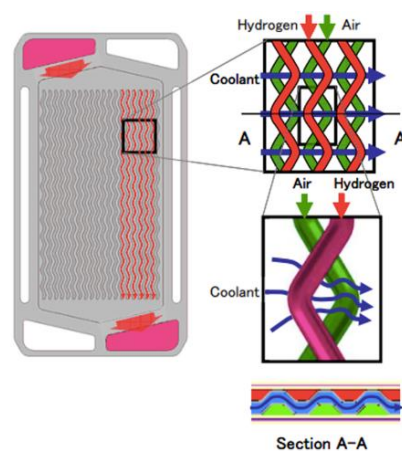


Figure 15. Design of coolant channels in the Honda FCX Clarity Fuel Cell [112].

New perspectives in the search for alternative cooling systems are represented by nanofluids, heat pipes, edge cooling, phase change materials (PCM), metal hydrides, and better integration with fuel cell water management [112].

The thermal management system is not only used for heat removal, but it also represents a way to provide the necessary heat for start-up in cold conditions. Below $0\text{ }^{\circ}\text{C}$, water will freeze, reducing the reaction surface and reactant transport. Chen et al. [112] report cooling methods and cold start-up capabilities for different water-cooled FCEVs, usually around $-30\text{ }^{\circ}\text{C}$.

Finally, the thermal management system can also be used for preheating the gaseous reactants through heat recovery and reutilization of waste heat where needed in a co-generative manner [112]. Wang et al. [63] illustrated the pros and cons of the principal cooling methods.

5. Energy Management System

FCEVs are an assembly of multiple systems that must be managed in an integrated and comprehensive way in order to reach and maintain optimal working conditions. Hybrid vehicles must include a system capable of integrating the power flows from the fuel cell, the battery, and the possibly installed supercapacitors at the different power loads. Those energy management strategies should be designed to minimize hydrogen consumption, sustain the energy storage system (ESS) charge, and maximize the lifespan of the different components, especially the fuel cell, which represents the main concern for the durability of the vehicle. Indeed, the frequent start and stop cycles, varying loads, and low- and high-power operation are demanding conditions potentially harmful for the fuel cell. Water management is an essential aspect of minimizing those problems [114].

The first control level is represented by the energy management system (EMS), which, by using appropriate algorithms, can perform load distribution and split the power request among the different energy and power sources of the vehicle. This system also controls the connected behavior of the fuel cell and the on-board energy storage systems, deciding whether it is appropriate to use the fuel cell to recharge them. It also addresses the recharging power flows during regenerative braking [21].

Secondly, low-level controllers (i.e., fuel cell controllers) regulate the different parameters of the different power sources (i.e., in the case of a fuel cell, reactant flows, humidification, cooling, etc.) to comply with the requests set by the energy management system [21].

Sorlei et al. [21] give an overview of the main control strategies used in FCEVs, as well as the principal advantages and disadvantages of the different approaches. Those strategies are briefly summarized below:

- **Rule-Based Strategies:** This type of control is based on predefined functions, set according to the knowledge of the system, the operating conditions, and the desired performance. Its implementation is relatively simple but not very adaptable: the results are not always accurate since the driving conditions can strongly influence the different parameters of the pre-established functions;
- **Optimization-based strategy:** It uses specific algorithms to find the optimal operating point of the various control parameters to optimize specific objectives, taking into account pre-established constraints. For example, optimizing fuel consumption, minimizing a specific cost function, etc. These algorithms can consider different variables and constraints simultaneously, at the expense of greater computational effort. By using this strategy, real-time information can be conveniently taken into account;
- **Learning Based Strategies:** It makes use of databases containing historical and real-time data for different driving conditions. This data can also be integrated into a model that optimizes power flows and overall performance. The main difference between the other strategies is their ability to learn using updated datasets.

6. Stack System Efficiency

The performance of a fuel cell depends on the performance of the stack and, as mentioned in the previous chapter, on that of the BoP.

The loss of efficiency of the stack can be represented as voltage drops across the cell, also called polarization. The origin of cell polarization can be traced back to three phenomena [62]:

1. **Activation polarization:** it is linked to the energy barrier that must be overcome for the redox reaction to take place. Its entity is related to the rate of electrode reactions;
2. **Concentration or mass transport polarization:** it is due to mass transport phenomena that hinder the reactions at the electrodes (diffusion of the reactant gases through the electrodes, solution and dissolution of reactants and products inside and outside the electrolyte);
3. **Ohmic Polarization:** it is caused by resistance to the flow of ions in the electrolyte and the flow of electrons through the electrode materials.

The trend of the overall voltage drop determined by the sum of these three components, also called cell polarization, can be visualized in the polarization curve in Figure 16a. Generally, the maximum efficiency values of fuel cell stacks for vehicular applications are around 60% [14]. This efficiency varies, firstly, with the current required by the load, decreasing as the current intensity increases. Furthermore, it depends on the multiple variables that influence the three polarizations described above: gas supply pressures, temperature, humidity, reaction kinetics, material characteristics, etc.

To evaluate the total efficiency of the system, another decisive factor to be taken into consideration is the efficiency of the auxiliary systems. In addition to the intrinsic characteristics of the cell, the performance of a stack also depends, as described in the previous chapter, on the operating parameters of the BoP.

Figure 16b shows the typical power and efficiency curves of the stack and the fuel cell system. As can be seen from the efficiency curve; the best operating point is for moderate currents.

The efficiency losses due to the BoP power supply are mainly due to the energy consumption of the air compressor in the cathode circuit and, to a lesser extent, to the refrigeration circuit pump and any blower for hydrogen recirculation, if present.

Recent experiments in the automotive industry [88,89] showed that these losses, which vary according to the load and the operating conditions, can be in the order of 10% of the LHV of hydrogen. J. Sery et al. (2022) [88] report different graphs showing the trend of energy consumption by component of the BoP, the discrepancy between stack efficiency and system efficiency (including the BoP), and the effects of operating conditions such as temperature.

However, very few studies are present in the literature regarding the contribution of losses due to BoP in vehicular applications of fuel cell systems. Further research could therefore be the object of this line of activity.

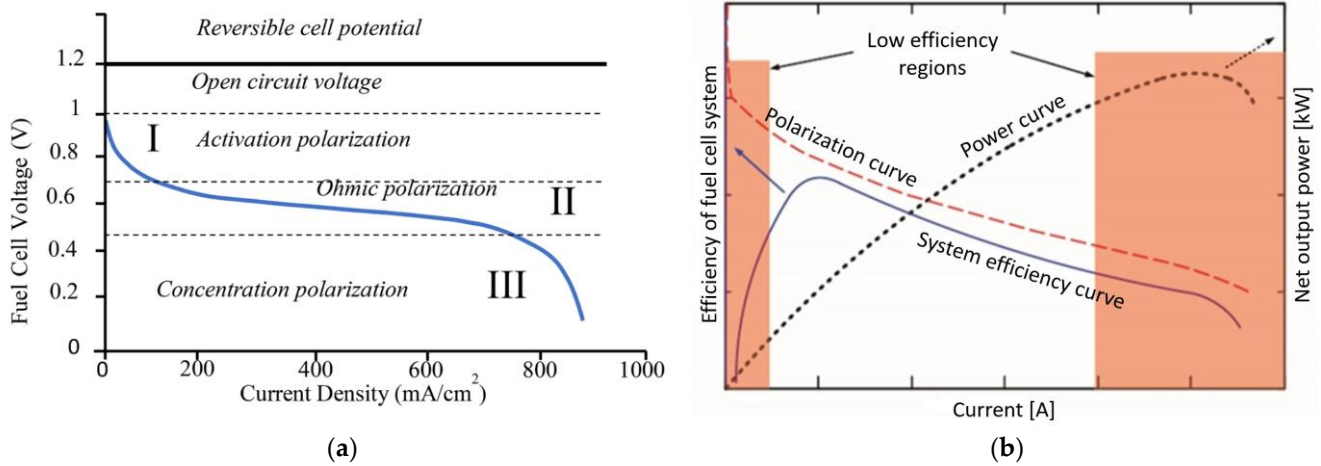


Figure 16. (a) The polarization curve of a fuel cell [115]. (b) Efficiency, power, and polarization curves of a PEM fuel cell [116].

7. Conclusions

PEM fuel cells are the most promising technology for vehicle hydrogen propulsion. The state-of-the-art PEM fuel cell technology and its BoP are outlined in this review. New research lines, alternative materials, and designs are also described. Many references were suggested to guide the readers through the landscape of hydrogen–electric mobility.

Furthermore, this work described the possible configurations of FCEVs and also analyzed the principal benefits and drawbacks of FCEVs in comparison with BEVs.

FCEVs can play a decisive role in reducing emissions from transport activities and accelerating the decarbonization process, especially with reference to sectors such as heavy-duty vehicles. However, this is only possible on the assumption that future energy systems will provide sufficient green energy to produce hydrogen.

Expansion of this sector is most likely expected; however, further efforts are necessary to cope with the many criticalities still present, such as the durability of the PEM fuel cells, cost, lack of infrastructure for hydrogen as a transportation fuel, and low well-to-wheel efficiency.

Author Contributions: Conceptualization, A.N.M. and C.M.; methodology, A.N.M. and C.M.; formal analysis, A.N.M.; investigation, A.N.M.; data curation, A.N.M.; writing—original draft preparation, A.N.M.; writing—review and editing, C.M., F.V., R.B. and M.P.; supervision, C.M., F.V., R.B. and M.P. All authors have read and agreed to the published version of the manuscript.

Funding: This research was funded by the European Union—NextGenerationEU from the Italian Ministry of Environment and Energy Security, POR H2 AdP MEES/ENEA with the involvement of CNR and RSE, PNRR—Mission 2, Component 2, Investment 3.5 “Ricerca e sviluppo sull’idrogeno”, CUP: I83C22001170006.

Data Availability Statement: No new data were created or analyzed in this study. Data sharing is not applicable to this article.

Conflicts of Interest: The authors declare no conflict of interest.

References

1. Vatsalya Sohu. The Outlook for Transport: Speedy Recovery, New Uncertainties. In *ITF Transport Outlook 2023*; International Transport Forum, OECD: Paris, France, 2023; Chapter 1. [CrossRef]
2. Global CO₂ Emissions in Transport by Mode in the Sustainable Development Scenario, 2000–2070. IEA: Paris, France. 2020. Available online: <https://www.iea.org/data-and-statistics/charts/global-co2-emissions-in-transport-by-mode-in-the-sustainable-development-scenario-2000-2070> (accessed on 24 July 2023).
3. Ocktaeck, L. Fuel Cell Electric Vehicles. In *Hybrid and Electric Vehicles—The Electric Drive Automates*; Task 35; Meyer, G., Ed.; International Energy Agency: Paris, France, 2018.
4. HEV TCP Annual Report 2023. Available online: https://ieahev.org/wp-content/uploads/2023/06/Digital_HEVTCP_Annual_Report_2023_v0.3-3.pdf (accessed on 24 July 2023).
5. IEA. Global EV Policy Explorer. Available online: <https://www.iea.org/data-and-statistics/data-tools/global-ev-policy-explorer> (accessed on 26 April 2023).
6. Basma, H.; Rodríguez, F. *Fuel Cell Electric Tractor-Trailers: Technology Overview and Fuel Economy*; Working Paper 2022-23; International Council On Clean Transportation: Washington, DC, USA, 2022.
7. Council of the EU. Fit for 55 Package: Council Reaches General Approaches Relating to Emissions Reductions and Their Social Impacts. 29 June 2022. Available online: <https://www.consilium.europa.eu/en/press/press-releases/2022/06/29/fit-for-55-council-reaches-general-approaches-relating-to-emissions-reductions-and-removals-and-their-social-impacts/> (accessed on 24 July 2023).
8. IEA. Trends and developments in EV markets. In *Global EV Outlook 2023: Catching up with Climate Ambitions*; IEA: Paris, France, 2023.
9. Amending Regulation (EU) 2019/1242. 2023. Available online: <https://eur-lex.europa.eu/legal-content/EN/TXT/?uri=COM%3A2023%3A88%3AFIN> (accessed on 24 July 2023).
10. Requia, W.J.; Mohamed, M.; Higgins, C.D.; Arain, A.; Ferguson, M. How clean are electric vehicles? Evidence-based review of the effects of electric mobility on air pollutants, greenhouse gas emissions and human health. *Atmos. Environ.* **2018**, *185*, 64–77. [CrossRef]
11. Zhang, H.; Sun, C.; Ge, M. Review of the Research Status of Cost-Effective Zinc–Iron Redox Flow Batteries. *Batteries* **2022**, *8*, 202. [CrossRef]
12. Gils, H.C.; Gardian, H.; Schmutz, J. Interaction of hydrogen infrastructures with other sector coupling options towards a zero-emission energy system in Germany. *Renew. Energy* **2021**, *180*, 140–156. [CrossRef]
13. Aminudin, M.A.; Kamarudin, S.K.; Lim, B.H.; Majilan, E.H.; Masdar, M.S.; Shaari, N. An overview: Current progress on hydrogen fuel cell vehicles. *Int. J. Hydrogen Energy* **2023**, *48*, 4371–4388. [CrossRef]
14. Cullen, D.A.; Neyerlin, K.C.; Ahluwalia, R.K.; Mukundan, R.; More, K.L.; Borup, R.L.; Weber, A.Z.; Myers, D.J.; Kusoglu, A. New roads and challenges for fuel cells in heavy-duty transportation. *Nat. Energy* **2021**, *6*, 462–474. [CrossRef]
15. Wang, Y.; Seo, B.; Wang, B.; Zamel, N.; Jiao, K.; Adroher, X.C. Fundamentals, materials, and machine learning of polymer electrolyte membrane fuel cell technology. *Energy AI* **2020**, *1*, 100014. [CrossRef]
16. Selmi, T.; Khadhraoui, A.; Cherif, A. Fuel cell-based electric vehicles technologies and challenges. *Environ. Sci. Pollut. Res.* **2022**, *29*, 78121–78131. [CrossRef]
17. Mekhilef, S.; Saidur, R.; Safari, A. Comparative study of different fuel cell technologies. *Renew. Sustain. Energy Rev.* **2012**, *16*, 981–989. [CrossRef]
18. Verma, S.; Mishra, S.; Gaur, A.; Chowdhury, S.; Mohapatra, S.; Dwivedi, G.; Verma, P. A comprehensive review on energy storage in hybrid electric vehicle. *J. Traffic Transp. Eng.* **2021**, *8*, 621–637. [CrossRef]
19. Das, H.S.; Tan, C.W.; Yatim, A.H.M. Fuel cell hybrid electric vehicles: A review on power conditioning units and topologies. *Renew. Sustain. Energy Rev.* **2017**, *76*, 268–291. [CrossRef]
20. Samsun, R.C.; Antoni, L.; Rex, M.; Stolten, D. Deployment Status of Fuel Cells in Road Transport: Update 2021. *Energy Environ.* **2021**, *542*, 37.
21. Sorlei, I.-S.; Bizon, N.; Thounthong, P.; Varlam, M.; Carcadea, E.; Culcer, M.; Iliescu, M.; Raceanu, M. Fuel Cell Electric Vehicles—A Brief Review of Current Topologies and Energy Management Strategies. *Energies* **2021**, *14*, 252. [CrossRef]
22. Pollet, B.G.; Kocha, S.S.; Staffell, I. Current status of automotive fuel cells for sustainable transport. *Curr. Opin. Electrochem.* **2019**, *16*, 90–95. [CrossRef]
23. Kleen, G.; Padgett, E. *Durability-Adjusted Fuel Cell System Cost*; U.S. Department of Energy: Washington, DC, USA, 2021. Available online: <https://www.hydrogen.energy.gov/pdfs/21001-durability-adjusted-fcs-cost.pdf> (accessed on 24 July 2023).
24. Zhang, T.; Wang, P.; Chen, H.; Pei, P. A review of automotive proton exchange membrane fuel cell degradation under start-stop operating condition. *Appl. Energy* **2018**, *223*, 249–262. [CrossRef]
25. Arrigoni, A.; Arosio, V.; Basso Peressut, A.; Latorrata, S.; Dotelli, G. Greenhouse Gas Implications of Extending the Service Life of PEM Fuel Cells for Automotive Applications: A Life Cycle Assessment. *Clean Technol.* **2022**, *4*, 132–148. [CrossRef]
26. Staffell, I.; Scamman, D.; Velazquez Abad, A.; Balcombe, P.; Dodds, P.E.; Ekins, P.; Shahd, N.; Warda, K.R. The role of hydrogen and fuel cells in the global energy system. *Energy Environ. Sci.* **2019**, *12*, 463–491. [CrossRef]
27. Genovese, M.; Fragiaco, P. Hydrogen refueling station: Overview of the technological status and research enhancement. *J. Energy Storage* **2023**, *61*, 106758. [CrossRef]

28. Thompson, S.T.; James, B.D.; Huya-Kouadio, J.M.; Houchins, C.; DeSantis, D.A.; Ahluwalia, R.; Wilson, A.R.; Kleen, G.; Papageorgopoulos, D. Direct hydrogen fuel cell electric vehicle cost analysis: System and high-volume manufacturing description, validation, and outlook. *J. Power Source* **2018**, *399*, 304–313. [[CrossRef](#)]
29. Olabi, A.G.; Abdelkareem, M.A.; Wilberforce, T.; Alami, A.H.; Alkhalidi, A.; Hassan, M.M.; Sayed, E.T. Strength, weakness, opportunities, and threats (SWOT) analysis of fuel cells in electric vehicles. *Int. J. Hydrogen Energy* **2023**, *48*, 23185–23211. [[CrossRef](#)]
30. Manoharan, Y.; Hosseini, S.E.; Butler, B.; Alzahrani, H.; Fou, B.T., Sr.; Ashuri, T.; Krohn, J. Hydrogen Fuel Cell Vehicles; Current Status and Future Prospect. *Appl. Sci.* **2019**, *9*, 2296. [[CrossRef](#)]
31. Habib, M.S.; Arefin, P.; Salam, M.A.; Ahmed, K.; Uddin, M.S.; Hossain, T.; Papri, N.; Islam, T. Proton Exchange Membrane Fuel Cell (PEMFC) Durability Factors, Challenges, and Future Perspectives: A Detailed Review. *Mat. Sci. Res. India* **2021**, *18*, 217–234. [[CrossRef](#)]
32. Luca, R.; Whiteley, M.; Neville, T.; Shearing, P.R.; Brett, D.J.L. Comparative study of energy management systems for a hybrid fuel cell electric vehicle—A novel mutative fuzzy logic controller to prolong fuel cell lifetime. *Int. J. Hydrogen Energy* **2022**, *47*, 24042–24058. [[CrossRef](#)]
33. Molina-Ibáñez, E.-L.; Rosales-Asensio, E.; Pérez-Molina, C.; Pérez, F.M.; Colmenar-Santos, A. Analysis on the electric vehicle with a hybrid storage system and the use of Superconducting magnetic energy storage (SMES). *Energy Rep.* **2021**, *7*, 854–873. [[CrossRef](#)]
34. Pardhi, S.; Chakraborty, S.; Tran, D.-D.; El Baghdadi, M.; Wilkins, S.; Hegazy, O. A Review of Fuel Cell Powertrains for Long-Haul Heavy-Duty Vehicles: Technology, Hydrogen, Energy and Thermal Management Solutions. *Energies* **2022**, *15*, 9557. [[CrossRef](#)]
35. Battery or Fuel Cell, That Is the Question, Volkswagen. 2020. Available online: <https://www.volkswagen-newsroom.com/en/stories/battery-or-fuel-cell-that-is-the-question-5868> (accessed on 24 July 2023).
36. Wilken, D.; Oswald, M.; Draheim, P.; Pade, C.; Brand, U.; Vogt, T. Multidimensional assessment of passenger cars: Comparison of electric vehicles with internal combustion engine vehicles. *Procedia CIRP* **2020**, *90*, 291–296. [[CrossRef](#)]
37. Thangavelautham, J. Degradation in PEM Fuel Cells and Mitigation Strategies Using System Design and Control. In *Proton Exchange Membrane Fuel Cell*; Taner, T., Ed.; IntechOpen: London, UK, 2018; Chapter 5.
38. Cano, Z.P.; Banham, D.; Ye, S.; Hintennach, A.; Lu, J.; Fowler, M.; Chen, Z. Batteries and fuel cells for emerging electric vehicle markets. *Nat. Energy* **2018**, *3*, 279–289. [[CrossRef](#)]
39. Tsakiris, A. Analysis of hydrogen fuel cell and battery efficiency. In Proceedings of the World Sustainable Energy Days 2019, Young Energy Researchers Conference, Wels, Austria, 27 February 2019.
40. Aghabali, I.; Bauman, J.; Kollmeyer, P.J.; Wang, Y.; Bilgin, B.; Emadi, A. 800-V Electric Vehicle Powertrains: Review and Analysis of Benefits, Challenges, and Future Trends. *IEEE Trans. Transp. Electrification* **2021**, *7*, 927–948. [[CrossRef](#)]
41. Anselma, P.G.; Belingardi, G. Fuel cell electrified propulsion systems for long-haul heavy-duty trucks: Present and future cost-oriented sizing. *Appl. Energy* **2022**, *321*, 119354. [[CrossRef](#)]
42. Thomas, C.E. Fuel cell and battery electric vehicles compared. *Int. J. Hydrogen Energy* **2009**, *34*, 6005–6020. [[CrossRef](#)]
43. Dirkes, S.; Leidig, J.; Fisch, P.; Pischinger, S. Prescriptive Lifetime Management for PEM fuel cell systems in transportation applications, Part I: State of the art and conceptual design. *Energy Convers. Manag.* **2023**, *277*, 116598. [[CrossRef](#)]
44. Verbruggen, F.; Hoekstra, A.; Hofman, T. Evaluation of the state-of-the-art of full-electric medium and heavy-duty trucks. In Proceedings of the 2018 World Electric Vehicle Symposium and Exhibition (EVS31), Kobe, Japan, 1–3 October 2018.
45. Kast, J.; Morrison, G.; Gangloff, J.J.; Vijaygopal, R.; Marcinkoski, J. Designing hydrogen fuel cell electric trucks in a diverse medium and heavy duty market. *Res. Transp. Econ.* **2018**, *70*, 139–147. [[CrossRef](#)]
46. Hao, H.; Geng, Y.; Tate, J.E.; Liu, F.; Sun, X.; Mu, Z.; Xun, D.; Liu, Z.; Zhao, F. Securing Platinum-Group Metals for Transport Low-Carbon Transition. *One Earth* **2019**, *1*, 117–125. [[CrossRef](#)]
47. Hao, H.; Geng, Y.; Tate, J.E.; Liu, F.; Chen, K.; Sun, X.; Liu, Z.; Zhao, F. Impact of transport electrification on critical metal sustainability with a focus on the heavy-duty segment. *Nat. Commun.* **2019**, *10*, 5398. [[CrossRef](#)]
48. Liu, F.; Mauzerall, D.L.; Zhao, F.; Hao, H. Deployment of fuel cell vehicles in China: Greenhouse gas emission reductions from converting the heavy-duty truck fleet from diesel and natural gas to hydrogen. *Int. J. Hydrogen Energy* **2021**, *46*, 17982–17997. [[CrossRef](#)]
49. Kane, M. Hydrogen Fuel Cell Car Sales in 2019 Improved to 7500 Globally. 2020. Available online: www.insideevs.com/news/397240/hydrogen-fuel-cell-sales-2019-7500-globally. (accessed on 24 July 2023).
50. Hyundai News. Hyundai Motor Group Reveals “FCEV Vision 2030”. 2018. Available online: <https://www.hyundai.news/eu/articles/press-releases/hyundai-motor-group-reveals-fcev-vision-2030.html> (accessed on 24 July 2023).
51. Li, M.; Bai, Y.; Zhang, C.; Song, Y.; Jiang, S.; Grouset, D.; Zhang, M. Review on the research of hydrogen storage system fast refueling in fuel cell vehicle. *Int. J. Hydrogen Energy* **2019**, *44*, 10677–10693. [[CrossRef](#)]
52. Sinha, P.; Brophy, B. Life cycle assessment of renewable hydrogen for fuel cell passenger vehicles in California. *Sustain. Energy Technol. Assess.* **2021**, *45*, 101188. [[CrossRef](#)]
53. Automotive News Europe. Daimler Will end Development of Fuel Cell Cars, 22 April 2020. Available online: <https://europe.autonews.com/automakers/daimler-will-end-development-fuel-cell-cars> (accessed on 24 July 2023).
54. Fuel Cell Electric Buses Knowledge Base, Fuel Cell Electric Buses. Available online: <https://www.fuelcellbuses.eu/> (accessed on 24 July 2023).

55. Yartys, V.A.; Lototsky, M.V.; Linkov, V.; Pasupathi, S.; Davids, M.W.; Tolj, I.; Radica, G.; Denys, R.V.; Eriksen, J.; Taube, K.; et al. HYDRIDE4MOBILITY: An EU HORIZON 2020 project on hydrogen powered fuel cell utility vehicles using metal hydrides in hydrogen storage and refuelling systems. *Int. J. Hydrogen Energy* **2021**, *46*, 35896–35909. [CrossRef]
56. Kenworth. T680 Fuel Cell Electric Vehicle. Available online: <https://www.kenworth.com/trucks/t680-fcev/> (accessed on 11 August 2023).
57. Nikola Corp. TRE FCEV. All Science. No Fiction. Available online: <https://www.nikolamotor.com/tre-fcev/> (accessed on 11 August 2023).
58. Lin, C.-W.; Chien, C.-H.; Tan, J.; Chao, Y.-J.; Van Zee, J.W. Dynamic mechanical characteristics of five elastomeric gasket materials aged in a simulated and an accelerated PEM fuel cell environment. *Int. J. Hydrogen Energy* **2011**, *36*, 6756–6767. [CrossRef]
59. Pei, P.; Wang, M.; Chen, D.; Ren, P.; Zhang, L. Key technologies for polymer electrolyte membrane fuel cell systems fueled impure hydrogen. *Prog. Nat. Sci. Mater. Int.* **2020**, *30*, 751–763. [CrossRef]
60. Benmouiza, K.; Cheknane, A. Analysis of proton exchange membrane fuel cells voltage drops for different operating parameters. *Int. J. Hydrogen Energy* **2018**, *43*, 3512–3519. [CrossRef]
61. Rezk, H.; Wilberforce, T.; Olabi, A.G.; Ghoniem, R.M.; Sayed, E.T.; Ali Abdelkareem, M. Optimal Parameter Identification of a PEM Fuel Cell Using Recent Optimization Algorithms. *Energies* **2023**, *16*, 5246. [CrossRef]
62. Pourrahmani, H.; Siavashi, M.; Yavarinasab, A.; Matian, M.; Chitgar, N.; Wang, L.; Van herle, J. A Review on the Long-Term Performance of Proton Exchange Membrane Fuel Cells: From Degradation Modeling to the Effects of Bipolar Plates, Sealings, and Contaminants. *Energies* **2022**, *15*, 5081. [CrossRef]
63. Wang, Y.; Ruiz Diaz, D.F.; Chen, K.S.; Wang, Z.; Adroher, X.C. Materials, technological status, and fundamentals of PEM fuel cells—A review. *Mater. Today* **2020**, *32*, 178–203. [CrossRef]
64. Zelovich, T.; Winey, K.I.; Tuckerman, M.E. Hydronium ion diffusion in model proton exchange membranes at low hydration: Insights from ab initio molecular dynamics. *J. Mater. Chem. A* **2021**, *9*, 2448–2458. [CrossRef]
65. Banerjee, S. *Handbook of Specialty Fluorinated Polymers: Preparation, Properties, and Applications*; Elsevier William Andrew: Waltham, MA, USA, 2015.
66. Chen, P.; Fang, F.; Zhang, Z.; Zhang, W.; Wang, Y. Self-assembled graphene film to enable highly conductive and corrosion resistant aluminum bipolar plates in fuel cells. *Int. J. Hydrogen Energy* **2017**, *42*, 12593–12600. [CrossRef]
67. Rosli, N.A.H.; Loh, K.S.; Wong, W.Y.; Yunus, R.M.; Lee, T.K.; Ahmad, A.; Chong, S.T. Review of Chitosan-Based Polymers as Proton Exchange Membranes and Roles of Chitosan-Supported Ionic Liquids. *Int. J. Mol. Sci.* **2020**, *21*, 632. [CrossRef]
68. Chen, C.-Y.; Su, J.-H.; Ali, H.M.; Yan, W.-M.; Amani, M. Effect of channel structure on the performance of a planar membrane humidifier for proton exchange membrane fuel cell. *Int. J. Heat Mass Transf.* **2020**, *163*, 120522. [CrossRef]
69. Shao, M.; Chang, Q.; Dodelet, J.-P.; Chenitz, R. Recent Advances in Electrocatalysts for Oxygen Reduction Reaction. *Chem. Rev.* **2016**, *116*, 3594–3657. [CrossRef]
70. Popov, B.N.; Ho, D.; Benjamin, T. V.A.6 *Development of Ultra-Low Platinum Alloy Cathode Catalysts for PEM Fuel Cells*; FY 2015 Annual Progress Report; Univ. of South Carolina: Columbia, SC, USA, 2015.
71. Wang, Y.; Yu, J.; Wu, J.; Wang, Z. Rapid Analysis of Platinum and Nafion Loadings Using Laser Induced Breakdown Spectroscopy. *J. Electrochem. Soc.* **2017**, *164*, F1294–F1300. [CrossRef]
72. Sharma, J.; Lyu, X.; Reshetyenko, T.; Polizos, G.; Livingston, K.; Li, J.; Wood, D.L.; Serov, A. Catalyst layer formulations for slot-die coating of PEM fuel cell electrodes. *Int. J. Hydrogen Energy* **2022**, *47*, 35838–35850. [CrossRef]
73. Borup, R.L.; Mukundan, R.; More, K.L.; Neyerlin, K.C.; Weber, A.; Myers, D.J.; Ahluwalia, R. PEM Fuel Cell Catalyst Layer (MEA) Architectures. In Proceedings of the Electrochemical Society Conference, Seattle, WA, USA, 13 May 2018. Available online: <https://www.osti.gov/biblio/1440415> (accessed on 24 July 2023).
74. Borup, R.L.; More, K.L.; Myers, D.J. FC-PAD: Fuel Cell Performance and Durability Consortium Update to USCAR Analysis of Toyota Mirai Components Provided by USCAR. In Proceedings of the USCAR, Southfield, MI, USA, 11 May 2018. Available online: <https://www.osti.gov/servlets/purl/1440417> (accessed on 11 August 2023).
75. Jaouen, F.; Jones, D.; Coutard, N.; Artero, V.; Strasser, P.; Kucernak, A. Toward Platinum Group Metal-Free Catalysts for Hydrogen/Air Proton-Exchange Membrane Fuel Cells. *Johns. Matthey Technol. Rev.* **2018**, *62*, 231–255. [CrossRef]
76. Bai, Z.; Huang, R.; Niu, L.; Zhang, Q.; Yang, L.; Zhang, J. A Facile Synthesis of Hollow Palladium/Copper Alloy Nanocubes Supported on N-Doped Graphene for Ethanol Electrooxidation Catalyst. *Catalysts* **2015**, *5*, 747–758. [CrossRef]
77. Haug, A.; Zenyuk, I.; Allen, J.; Lindell, M.; Sun, F.; Abulu, J.; Yandrasits, M.; Thoma, G.; Steinbach, A.; Kurkowski, M.; et al. *Novel Ionomers and Electrode Structures for Improved PEMFC Electrode Performance at Low PGM Loadings (Final Report)*; 3M Company: Maplewood, MN, USA, 2020. [CrossRef]
78. Pintauro, P. Fuel Cell Membrane-Electrode-Assemblies with Ultra-Low Pt Nanofiber Electrodes. DOE Hydrogen and Fuel Cells Program. Annual Progress Report. 2018. Available online: https://www.hydrogen.energy.gov/pdfs/progress18/fc_pintauro_2018.pdf (accessed on 24 July 2023).
79. Wu, G. Current challenge and perspective of PGM-free cathode catalysts for PEM fuel cells. *Front. Energy* **2017**, *11*, 286–298. [CrossRef]
80. Banham, D.; Ye, S. Current Status and Future Development of Catalyst Materials and Catalyst Layers for Proton Exchange Membrane Fuel Cells: An Industrial Perspective. *ACS Energy Lett.* **2017**, *2*, 629–638. [CrossRef]

81. Cui, R.; Mei, L.; Han, G.; Chen, J.; Zhang, G.; Quan, Y.; Gu, N.; Zhang, L.; Fang, Y.; Qian, B.; et al. Facile Synthesis of Nanoporous Pt-Y alloy with Enhanced Electrocatalytic Activity and Durability. *Sci. Rep.* **2017**, *7*, 41826. [CrossRef]
82. Zhang, J.; Wang, B.; Jin, J.; Yang, S.; Li, G. A review of the microporous layer in proton exchange membrane fuel cells: Materials and structural designs based on water transport mechanism. *Renew. Sustain. Energy Rev.* **2022**, *156*, 111998. [CrossRef]
83. Malekian, A.; Salari, S.; Stumper, J.; Djilali, N.; Bahrami, M. Effect of compression on pore size distribution and porosity of PEM fuel cell catalyst layers. *Int. J. Hydrogen Energy* **2019**, *44*, 23396–23405. [CrossRef]
84. Alo, O.A.; Otunniyi, I.O.; Pienaar, H.; Iyuke, S.E. Materials for Bipolar Plates in Polymer Electrolyte Membrane Fuel Cell: Performance Criteria and Current Benchmarks. *Procedia Manuf.* **2017**, *7*, 395–401. [CrossRef]
85. Neto, D.M.; Oliveira, M.C.; Alves, J.L.; Menezes, L.F. Numerical Study on the Formability of Metallic Bipolar Plates for Proton Exchange Membrane (PEM) Fuel Cells. *Metals* **2019**, *9*, 810. [CrossRef]
86. Baumann, N.; Blankenship, A.; Dorn, M.; Cremers, C. Evaluating Current Distribution and Influence of Defect Sites for Graphitic Compound Bipolar Plate Materials. *Fuel Cells* **2020**, *20*, 40–47. [CrossRef]
87. Wei, H.; Du, C. Active Disturbance Rejection-Based Performance Optimization and Control Strategy for Proton-Exchange Membrane Fuel Cell System. *Electronics* **2023**, *12*, 1393. [CrossRef]
88. Sery, J.; Leduc, P. Fuel cell behavior and energy balance on board a Hyundai Nexa. *Int. J. Engine Res.* **2022**, *23*, 709–720. [CrossRef]
89. Lohse-Busch, H.; Stutenberg, K.; Duoba, M.; Liu, X.; Elgowainy, A.; Wang, M.; Wallner, T.; Richard, B.; Christenson, M. Automotive fuel cell stack and system efficiency and fuel consumption based on vehicle testing on a chassis dynamometer at minus 18 °C to positive 35 °C temperatures. *Int. J. Hydrogen Energy* **2020**, *45*, 861–872. [CrossRef]
90. Zhao, Y.; Liu, Y.; Liu, G.; Yang, Q.; Li, L.; Gao, Z. Air and hydrogen supply systems and equipment for PEM fuel cells: A review. *Int. J. Green Energy* **2022**, *19*, 331–348. [CrossRef]
91. Martinez-Boggio, S.; Di Blasio, D.; Fletcher, T.; Burke, R.; García, A.; Monsalve-Serrano, J. Optimization of the air loop system in a hydrogen fuel cell for vehicle application. *Energy Convers. Manag.* **2023**, *283*, 116911. [CrossRef]
92. Hoeflinger, J.; Hofmann, P. Air mass flow and pressure optimisation of a PEM fuel cell range extender system. *Int. J. Hydrogen Energy* **2020**, *45*, 29246–29258. [CrossRef]
93. Hou, J.; Yang, M.; Ke, C.; Zhang, J. Control logics and strategies for air supply in PEM fuel cell engines. *Appl. Energy* **2020**, *269*, 115059. [CrossRef]
94. Yin, X.; Wang, X.; Wang, L.; Qin, B.; Liu, H.; Jia, L.; Cai, W. Cooperative control of air and fuel feeding for PEM fuel cell with ejector-driven recirculation. *Appl. Therm. Eng.* **2021**, *199*, 117590. [CrossRef]
95. Su, H.; Ye, D.; Cai, Y.; Guo, W. Air starvation of proton exchange membrane fuel cells and its beneficial effects on performance. *Appl. Energy* **2022**, *323*, 119626. [CrossRef]
96. Gomez, A.; Sasmito, A.P.; Shamim, T. Investigation of the purging effect on a dead-end anode PEM fuel cell-powered vehicle during segments of a European driving cycle. *Energy Convers. Manag.* **2015**, *106*, 951–957. [CrossRef]
97. Macauley, N.; Watson, M.; Lauritzen, M.; Knights, S.; Wang, G.G.; Kjeang, E. Empirical membrane lifetime model for heavy duty fuel cell systems. *J. Power Source* **2016**, *336*, 240–250. [CrossRef]
98. Carcadea, E.; Ismail, M.S.; Ingham, D.B.; Patularu, L.; Schitea, D.; Marinoiu, A.; Ion-Ebrasu, D.; Mocanu, D.; Varlam, M. Effects of geometrical dimensions of flow channels of a large-active-area PEM fuel cell: A CFD study. *Int. J. Hydrogen Energy* **2021**, *46*, 13572–13582. [CrossRef]
99. Zhang, Y.; Xu, S.; Lin, C. Performance improvement of fuel cell systems based on turbine design and supercharging system matching. *Appl. Therm. Eng.* **2020**, *180*, 115806. [CrossRef]
100. Cruz Rojas, A.; Lopez Lopez, G.; Gomez-Aguilar, J.; Alvarado, V.; Sandoval Torres, C. Control of the Air Supply Subsystem in a PEMFC with Balance of Plant Simulation. *Sustainability* **2017**, *9*, 73. [CrossRef]
101. U.S. Department of Energy, Office of Energy Efficiency and Renewable Energy. Funding Opportunity Announcement (FOA), (EERE) DE-FOA0002022. 2019. Available online: <https://eere-exchange.energy.gov/Default.aspx?foaId=600decec-1f68-4c10-bda1-9ed3aad0735> (accessed on 24 July 2023).
102. Hydrogen Storage, U.S. Department of Energy—The Office of Energy Efficiency and Renewable Energy. Available online: <https://www.energy.gov/eere/fuelcells/hydrogen-storage#:~:text=Onboard%20hydrogen%20storage%20capacities%20of,of%20light%2Dduty%20vehicle%20platforms> (accessed on 24 July 2023).
103. Davoodabadi, A.; Mahmoudi, A.; Ghasemi, H. The potential of hydrogen hydrate as a future hydrogen storage medium. *iScience* **2021**, *24*, 101907. [CrossRef] [PubMed]
104. Frank, E.D.; Elgowainy, A.; Khalid, Y.S.; Peng, J.-K.; Reddi, K. Refueling-station costs for metal hydride storage tanks on board hydrogen fuel cell vehicles. *Int. J. Hydrogen Energy* **2019**, *44*, 29849–29861. [CrossRef]
105. Lototsky, M.V.; Tolj, I.; Pickering, L.; Sita, C.; Barbir, F.; Yartys, V. The use of metal hydrides in fuel cell applications. *Prog. Nat. Sci. Mater. Int.* **2017**, *27*, 3–20. [CrossRef]
106. Lototsky, M.V.; Tolj, I.; Parsons, A.; Smith, F.; Sita, C.; Linkov, V. Performance of electric forklift with low-temperature polymer exchange membrane fuel cell power module and metal hydride hydrogen storage extension tank. *J. Power Source* **2016**, *316*, 239–250. [CrossRef]
107. Singer, G.; Gappmayer, G.; Macherhammer, M.; Pertl, P.; Trattner, A. A development toolchain for a pulsed injector-ejector unit for PEM fuel cell applications. *Int. J. Hydrogen Energy* **2022**, *47*, 23818–23832. [CrossRef]

108. Chiche, A.; Lindbergh, G.; Stenius, I.; Lagergren, C. Design of experiment to predict the time between hydrogen purges for an air-breathing PEM fuel cell in dead-end mode in a closed environment. *Int. J. Hydrogen Energy* **2021**, *46*, 13806–13817. [[CrossRef](#)]
109. James, B.; Juya-Kouadio, J.; Houchins, C. Fuel Cell Systems Analysis. DOE Hydrogen and Fuel Cells Program Review FC163. 2017. Available online: https://www.hydrogen.energy.gov/pdfs/review17//fc163_james_2017_o.pdf (accessed on 24 July 2023).
110. Besagni, G.; Mereu, R.; Inzoli, F.; Chiesa, P. Application of an integrated lumped parameter-CFD approach to evaluate the ejector-driven anode recirculation in a PEM fuel cell system. *Appl. Therm. Eng.* **2017**, *121*, 628–651. [[CrossRef](#)]
111. Chen, J.; Li, J.; Zhou, D.; Zhang, H.; Weng, S. Control strategy design for a SOFC-GT hybrid system equipped with anode and cathode recirculation ejectors. *Appl. Therm. Eng.* **2018**, *132*, 67–79. [[CrossRef](#)]
112. Chen, Q.; Zhang, G.; Zhang, X.; Sun, C.; Jiao, K.; Wang, Y. Thermal management of polymer electrolyte membrane fuel cells: A review of cooling methods, material properties, and durability. *Appl. Energy* **2021**, *286*, 116496. [[CrossRef](#)]
113. Amirfazli, A.; Asghari, S.; Sarraf, M. An investigation into the effect of manifold geometry on uniformity of temperature distribution in a PEMFC stack. *Energy* **2018**, *145*, 141–151. [[CrossRef](#)]
114. Ferrara, A.; Jakubek, S.; Hametner, C. Energy management of heavy-duty fuel cell vehicles in real-world driving scenarios: Robust design of strategies to maximize the hydrogen economy and system lifetime. *Energy Convers. Manag.* **2021**, *232*, 113795. [[CrossRef](#)]
115. Mogorosi, K.; Oladiran, M.T.; Rakgati, E. Mathematical Modelling and Experimental Investigation of a Low Temperature Proton Exchange Membrane Fuel Cell. *EPE* **2020**, *12*, 653–670. [[CrossRef](#)]
116. Piatkowski, P.; Michalska-Pozoga, I.; Szczepanek, M. Fuel Cells in Road Vehicles. *Energies* **2022**, *15*, 8606. [[CrossRef](#)]

Disclaimer/Publisher’s Note: The statements, opinions and data contained in all publications are solely those of the individual author(s) and contributor(s) and not of MDPI and/or the editor(s). MDPI and/or the editor(s) disclaim responsibility for any injury to people or property resulting from any ideas, methods, instructions or products referred to in the content.